

## Zn-catalyzed *tert*-butyl nicotinate-directed amide cleavage as a biomimic of metallo-exopeptidase activity.

Clarence Chloë Daniëlla Wybon, Carl Mensch, Karlijn Hollanders, Charlène Gadais, Wouter A. Herrebout, Steven Ballet, and Bert U. W. Maes

ACS Catal., **Just Accepted Manuscript** • DOI: 10.1021/acscatal.7b02599 • Publication Date (Web): 14 Nov 2017

Downloaded from <http://pubs.acs.org> on November 14, 2017

### Just Accepted

“Just Accepted” manuscripts have been peer-reviewed and accepted for publication. They are posted online prior to technical editing, formatting for publication and author proofing. The American Chemical Society provides “Just Accepted” as a free service to the research community to expedite the dissemination of scientific material as soon as possible after acceptance. “Just Accepted” manuscripts appear in full in PDF format accompanied by an HTML abstract. “Just Accepted” manuscripts have been fully peer reviewed, but should not be considered the official version of record. They are accessible to all readers and citable by the Digital Object Identifier (DOI®). “Just Accepted” is an optional service offered to authors. Therefore, the “Just Accepted” Web site may not include all articles that will be published in the journal. After a manuscript is technically edited and formatted, it will be removed from the “Just Accepted” Web site and published as an ASAP article. Note that technical editing may introduce minor changes to the manuscript text and/or graphics which could affect content, and all legal disclaimers and ethical guidelines that apply to the journal pertain. ACS cannot be held responsible for errors or consequences arising from the use of information contained in these “Just Accepted” manuscripts.



1  
2  
3  
4  
5  
6  
7  
8  
9  
10  
11  
12  
13  
14  
15  
16  
17  
18  
19  
20  
21  
22  
23  
24  
25  
26  
27  
28  
29  
30  
31  
32  
33  
34  
35  
36  
37  
38  
39  
40  
41  
42  
43  
44  
45  
46  
47  
48  
49  
50  
51  
52  
53  
54  
55  
56  
57  
58  
59  
60

# Zn-catalyzed *tert*-butyl nicotinate-directed amide cleavage as a biomimic of metallo-exopeptidase activity

Clarence C. D. Wybon,<sup>†</sup> Carl Mensch,<sup>‡</sup> Karlijn Hollanders,<sup>†,¶</sup> Charlène Gadais,<sup>†,¶</sup>

Wouter A. Herrebout,<sup>‡</sup> Steven Ballet,<sup>¶</sup> and Bert U. W. Maes<sup>\*,†</sup>

<sup>†</sup>*Organic Synthesis, Department of Chemistry, University of Antwerp, Groenenborgerlaan 171, 2020  
Antwerp, Belgium*

<sup>‡</sup>*Molecular Spectroscopy, Department of Chemistry, University of Antwerp, Groenenborgerlaan 171,  
2020 Antwerp, Belgium*

<sup>¶</sup>*Organic Chemistry, Departments of Chemistry and Bioengineering Sciences, Vrije Universiteit  
Brussel, Pleinlaan 2, 1050 Brussels, Belgium*

E-mail: bert.maes@uantwerpen.be

## Abstract

A two-step catalytic amide-to-ester transformation of primary amides under mild reaction conditions has been developed. A *tert*-butyl nicotinate (*tBu nic*) directing group is easily introduced onto primary amides via Pd-catalyzed amidation with *tert*-butyl 2-chloronicotinate. A weak base (Cs<sub>2</sub>CO<sub>3</sub> or K<sub>2</sub>CO<sub>3</sub>) at 40–50 °C can be used provided 1,1'-bis(dicyclohexylphosphino)ferrocene is selected as ligand. The *tBu nic* activated amides subsequently allow Zn(OAc)<sub>2</sub>-catalyzed non-solvolytic alcoholysis in *tBuOAc* at 40–60 °C under neutral reaction conditions. The activation mechanism is biomimetic: the C3-ester substituent of the pyridine in the directing group populates the *trans*-conformer suitable for Zn-chelation, C=O<sub>amide</sub>-Zn-N<sub>directing group</sub>, and Zn-coordinated alcohol is additionally activated as a nucleophile by hydrogen bonding with the acetate ligand of the catalyst. Additionally, the acetate ligand assists in intramolecular *O*-to-*N* proton transfer. The chemoselectivity versus other functional groups and compatibility with challenging reaction partners, such as peptides, sugars and sterols, illustrates the synthetic applicability of this two-step amide cleavage method. The *tBu nic* amides do not require purification before cleavage. Preliminary experiments also indicate that other weak nucleophiles can be used such as (hetero)arylamines (transamidation) as exemplified by 8-aminoquinoline.

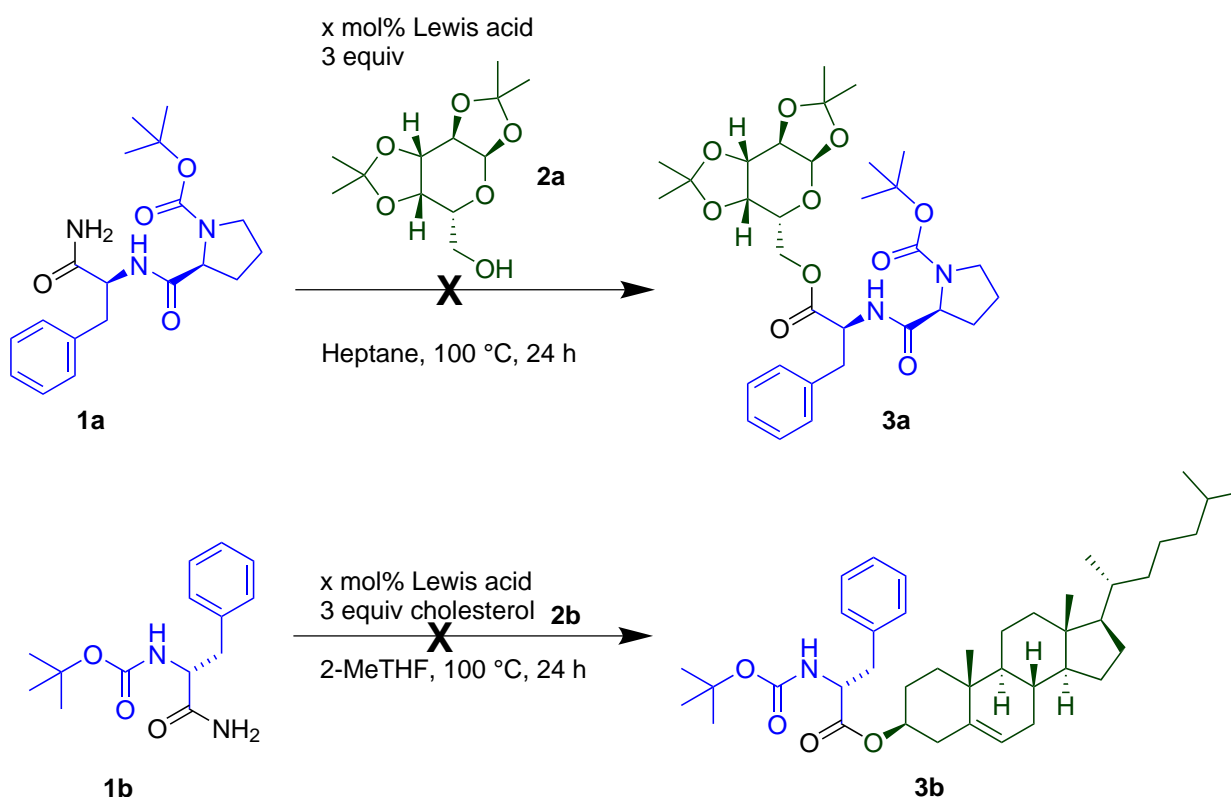
## Keywords

Amide cleavage, alcoholysis, esters, non-solvolytic, directing group, biomimicry, Pd-catalysis, Zn-catalysis

## Introduction

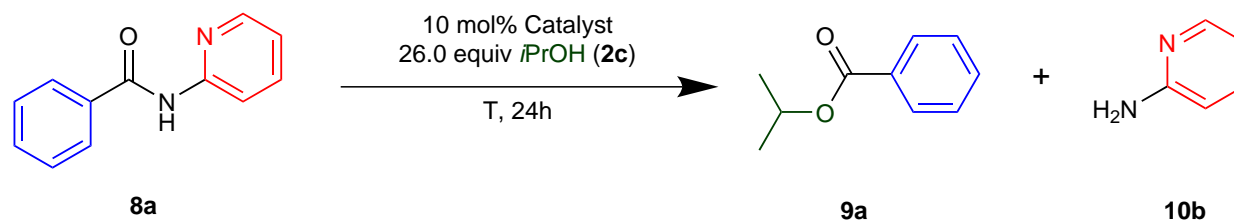
Amide functionalities are ubiquitous in natural products, agrochemicals and pharmaceuticals. They are crucial to sustain life, since these entities make up the peptide bonds in life-essential proteins such as enzymes. Therefore, amides can be considered as one of the most important functional groups in contemporary organic chemistry. In view of the prevalence of the amide functional group, and considering that nature has developed proteases to efficiently cleave them

under mild conditions, it is at first glance remarkable that the further synthetic transformation of this omnipresent structural entity has remained a challenging synthetic problem for organic chemists.<sup>1</sup> The reason for this can be found in the chemical inertness of the amide carbonyl towards nucleophilic addition.<sup>1,2</sup> A general transformation of amides into thermodynamically less stable esters is not a broadly accessible reaction for synthetic organic chemistry: amide esterification normally requires harsh conditions (strong (Lewis) acid or base and an elevated reaction temperature), with the alcohol standardly acting as both nucleophile and solvent.<sup>3,4</sup> These protocols often result in functional group compatibility problems and solvolytic nucleophile use limits the alcohol scope to liquids. The attempted reaction of Boc-L-Pro-L-Phe-NH<sub>2</sub> (**1a**) or Boc-D-Phe-NH<sub>2</sub> (**1b**) with a complex and solid alcohol (the sugar derivative diaceton- $\alpha$ -D-galactopyranose (**2a**) or cholesterol (**2b**)) in a solvent using different Lewis acids illustrates this is not a synthetically viable strategy (Scheme 1).



Scheme 1: Unsuccessful Lewis acid-catalyzed/mediated non-solvolytic cleavage of primary amides **1a** and **1b** with complex alcohols **2a** and **2b** ( $x$  mol% Lewis acid = 5 mol% Sc(OTf)<sub>2</sub>, 5 mol% Zn(OTf)<sub>2</sub>, 100 mol% BF<sub>3</sub>·Et<sub>2</sub>O).

Table 1: Selected catalyst screening in the solvolytic metal-catalyzed pyridine-directed cleavage of pyridin-2-ylbenzamide (**8a**) in *i*PrOH.



Entry	Catalyst	T (°C)	<b>8a</b> <sup>a,b</sup>	<b>9a</b> <sup>a,b</sup>
1	FeCl <sub>3</sub>	140	48	42
2	Fe(OAc) <sub>2</sub>	140	60	31
3	MnCl <sub>2</sub>	140	76	15
4	Mn(OAc) <sub>3</sub>	140	51	38
5	CuCl <sub>2</sub>	140	44	50
6	Cu(OAc) <sub>2</sub>	140	0	quant.
7	Cu(OAc) <sub>2</sub>	75	84	10
8	CoCl <sub>2</sub>	140	0	80
9	Co(OAc) <sub>2</sub>	140	1	96
10	Co(OAc) <sub>2</sub>	75	86	10
11	ZnCl <sub>2</sub>	140	37	62
12	ZnBr <sub>2</sub>	140	8	90
13	ZnBr <sub>2</sub>	75	74	23
14	Zn(OAc) <sub>2</sub>	140	0	quant.
15	Zn(OAc) <sub>2</sub>	75	72	25
16	NiCl <sub>2</sub> .DME <sup>c</sup>	140	63	5
17	Ni(OAc) <sub>2</sub>	140	4	89
18	Ni(OAc) <sub>2</sub>	75	86	5

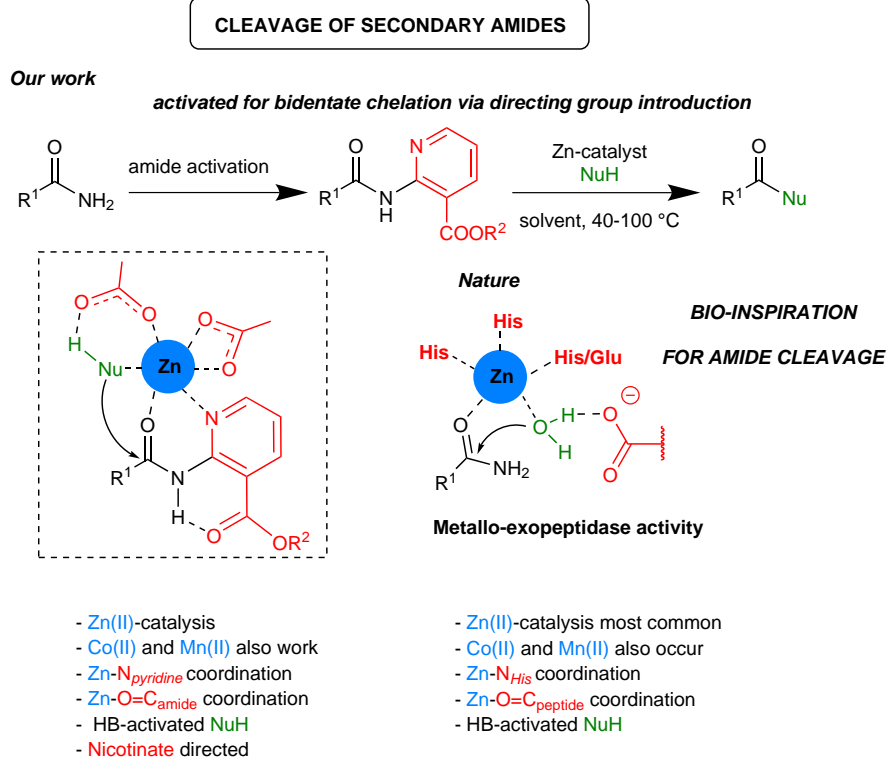
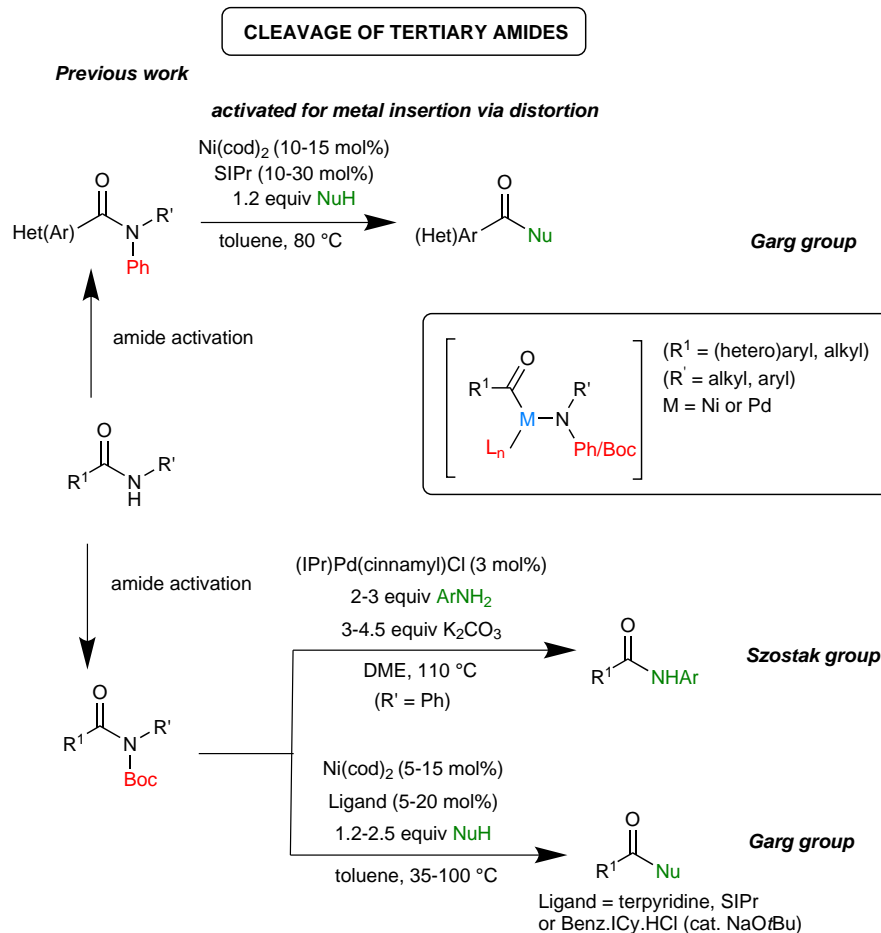
<sup>a</sup> 10 mol% catalyst, 26 equiv *i*PrOH, T, 24 h; <sup>b</sup> GC-yield with 1,3,5-trimethoxybenzene as internal standard; <sup>c</sup> Unselective reaction.

1  
2  
3  
4  
5  
6  
7  
8  
9  
10  
11  
12  
13  
14  
15  
16  
17  
18  
19  
20  
21  
22  
23  
24  
25  
26  
27  
28  
29  
30  
31  
32  
33  
34  
35  
36  
37  
38  
39  
40  
41  
42  
43  
44  
45  
46  
47  
48  
49  
50  
51  
52  
53  
54  
55  
56  
57  
58  
59  
60

However, this challenging amide transformation under mild conditions has a very interesting synthetic potential both in using amides as stable acyl precursors in multistep synthesis and in making new derivatives of readily available complex amides.<sup>5</sup> While transamidation with amines has been intensively studied,<sup>6</sup> strategies to allow direct amide-to-ester transformation with less nucleophilic alcohols are far less developed.<sup>1</sup> Distorted tertiary amides featuring reduced amide resonance have been reported to undergo cleavage with simple alcohols under low temperature conditions.<sup>1,7,8a</sup> Amide activation can also be achieved through metal chelation in the leaving group.<sup>8</sup> All these methods require specific amide substitution patterns and are typically based on solvolysis. Although these procedures represent very important conceptual advantages to tackle the alcoholysis problem, chemoselective amide alcoholysis featuring an easily introducible activating group applicable to a broad set of amides under mild reaction conditions with non-solvolytic alcohol remained an important synthetic challenge. Use of non-solvolytic alcohol is crucial to allow the use of more complex alcohols which are more expensive and often non-liquid (*vide supra*). In 2015 a Ni-catalyzed amide alcoholysis was reported,<sup>9a</sup> showing the first oxidative addition of the C-N bond of a distorted amide (Scheme 2).<sup>10</sup> Tertiary (hetero)arenecarboxamides featuring both a *N*-phenyl and *N*-alkyl group were suitable substrates for non-solvolytic alcoholysis at 80 °C.<sup>9a,11</sup> To extend the scope towards less reactive aliphatic amides, the Garg group recently disclosed that both a more activating *N*-Boc and a *N*-alkyl substituent were required in the substrate to allow alcoholysis at 100 °C (Scheme 2).<sup>9b</sup> These processes were subsequently extended to Ni-catalyzed transamidations with aliphatic amines (Scheme 2).<sup>12a,b,13</sup> More recently, more reactive Pd-catalyzed transamidations with challenging anilines were reported (Scheme 2).<sup>12c</sup> The nitrogen substituents in the tertiary amide are crucial to allow rate-determining oxidative addition of the C-N bond. Both types of amides, *N*-Ph-*N*-alkyl and *N*-Boc-*N*-alkyl, are activated for metal insertion via distortion which weakens the n(N)- $\pi^*(\text{C-O})$  conjugation.<sup>10</sup> Besides steric distortion, the phenyl or Boc enhances the amide reactivity through their electron withdrawing character. While the latter are non planar amides, the former are predominantly planar and activated by n(N)- $\pi^*(\text{Ar})$  delocalization.<sup>11b</sup> The Garg methodology is therefore ideal for the cleavage of secondary amides using a two-step protocol: Boc-group introduction followed by amide alcoholysis of the tertiary amide (Scheme 2). Likewise, it would be interesting to have access to a complementary methodology for

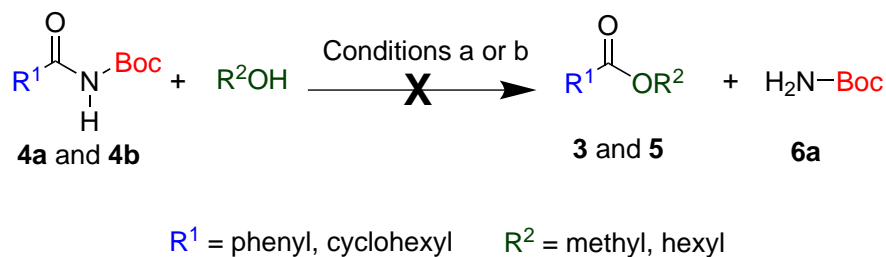
1  
2  
3 the alcoholysis of omnipresent carboxamide termini. Such a chemical transformation under mild  
4 non-solvolytic conditions is hitherto not available, but its development would extend the modern  
5 mild synthetic amide cleavage toolbox. Note that *N*-tert-butoxycarbonylation of a primary amide **1**  
6 (resulting in the formation of **4**), as used to activate secondary amides, does not provide a solution,  
7  
8 as application of the Ni-catalysis cleavage methodology on the resulting *N*-Boc secondary amide  
9  
10 **4a** and **4b** does not result in ester product **3** and **5** formation (Scheme 3). The only reaction that  
11  
12 occurs is *N*-Boc reductive cleavage of substrate. *N*-Boc removal is the major side-reaction typi-  
13  
14 cally observed in transition metal-catalyzed amide activation.<sup>13e</sup> Clearly, the N-H moiety present  
15  
16 requires another concept than amide distortion to increase its reactivity for mild cleavage using  
17  
18 limited excess of alcohol **2**. As Ni(0) is air-sensitive a method based on a transition metal in an  
19  
20 oxidation state compatible with air would be beneficial.  
21  
22  
23  
24

25  
26 Inspired by metallo-exopeptidases in nature,<sup>14</sup> we reasoned that an easily introducible directing  
27  
28 group (DG)<sup>15</sup> on the nitrogen atom of the primary amide, allowing bidentate chelation with a  
29  
30 transition metal might allow cleavage of a secondary amide under neutral and mild conditions  
31  
32 (Scheme 2). This directing group could biomimic<sup>16</sup> the His/Glu coordination with the metal  
33  
34 that activates the amide carbonyl in metalloproteases (C=O<sub>amide</sub>-M-(N<sub>His</sub>)<sub>n</sub>). Hydrogen bonding  
35  
36 activation of the nucleophile with the carboxylate side chain of Asp/Glu can be imitated by a ligand  
37  
38 of the metal catalyst, such as a carboxylate. A pyridin-2-yl (*py*) group was initially selected for this  
39  
40 purpose, as it should be easily introducible via transition metal-catalyzed amidation. However,  
41  
42 computational chemistry calculations on model substrate *N*-(pyridin-2-yl)benzamide (**8a**) showed  
43  
44 that less than 0.01% of **8a** exists in its *trans*-conformer **I**, with the amide carbonyl and DG  
45  
46 suitably oriented for bidentate chelation (Figure 1). We thus reasoned that a C3-*py*-substituent  
47  
48 might populate this desired conformer **I** through intramolecular hydrogen bonding with the amide  
49  
50 proton (in the case of a hydrogen bond acceptor (HBA) C3-substituent) and/or steric effects (size of  
51  
52 this C3-substituent). Interestingly, conformational analysis on a set of *N*-(C3-substituted pyridin-2-  
53  
54 yl)benzamides **8** revealed that several C3-groups allow population of the desired *trans*-conformer  
55  
56 **I** (Figure 1). C3-ester substituents were predicted to be superior for bidentate chelation with up  
57  
58 to 99% population of the desired *trans*-conformer **I** through intramolecular hydrogen bonding  
59  
60 with the amide proton (Scheme 2). Based on these conformer calculations we decided to study



Scheme 2: Ni- and Pd-catalyzed tertiary amide cleavage via secondary amide activation (top). Bio-inspired Zn-catalyzed secondary amide cleavage via primary amide activation (bottom).

substituted *N*-(pyridin-2-yl) groups as potentially suitable directing groups for mild metal-catalyzed non-solvolytic cleavage of primary amides with alcohols.



Conditions a ( $\text{R}^2 = \text{methyl}$ ): 10 mol%  $\text{Ni}(\text{cod})_2$ , 10 mol% SIPr, 1.2 equiv methanol (**2d**), toluene, 80 °C, 12 h (closed vial)

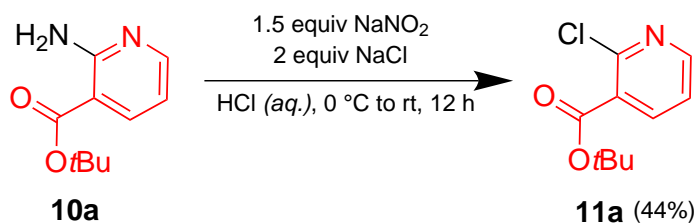
Conditions b ( $\text{R}^2 = \text{hexyl}$ ): 10 mol%  $\text{Ni}(\text{cod})_2$ , 10 mol% terpyridine, 1.25 equiv 1-hexanol (**2e**), toluene, 100 °C, 12 h (closed vial)

Scheme 3: Attempted Ni-catalyzed cleavage of Boc-activated primary amides **4** with alcohols **2** (SI S.5). SIPr = 1,3-Bis(2,6-diisopropylphenyl)-4,5-dihydroimidazol-2-ylidene, cod = 1,5-cyclooctadiene.

## Results and discussion

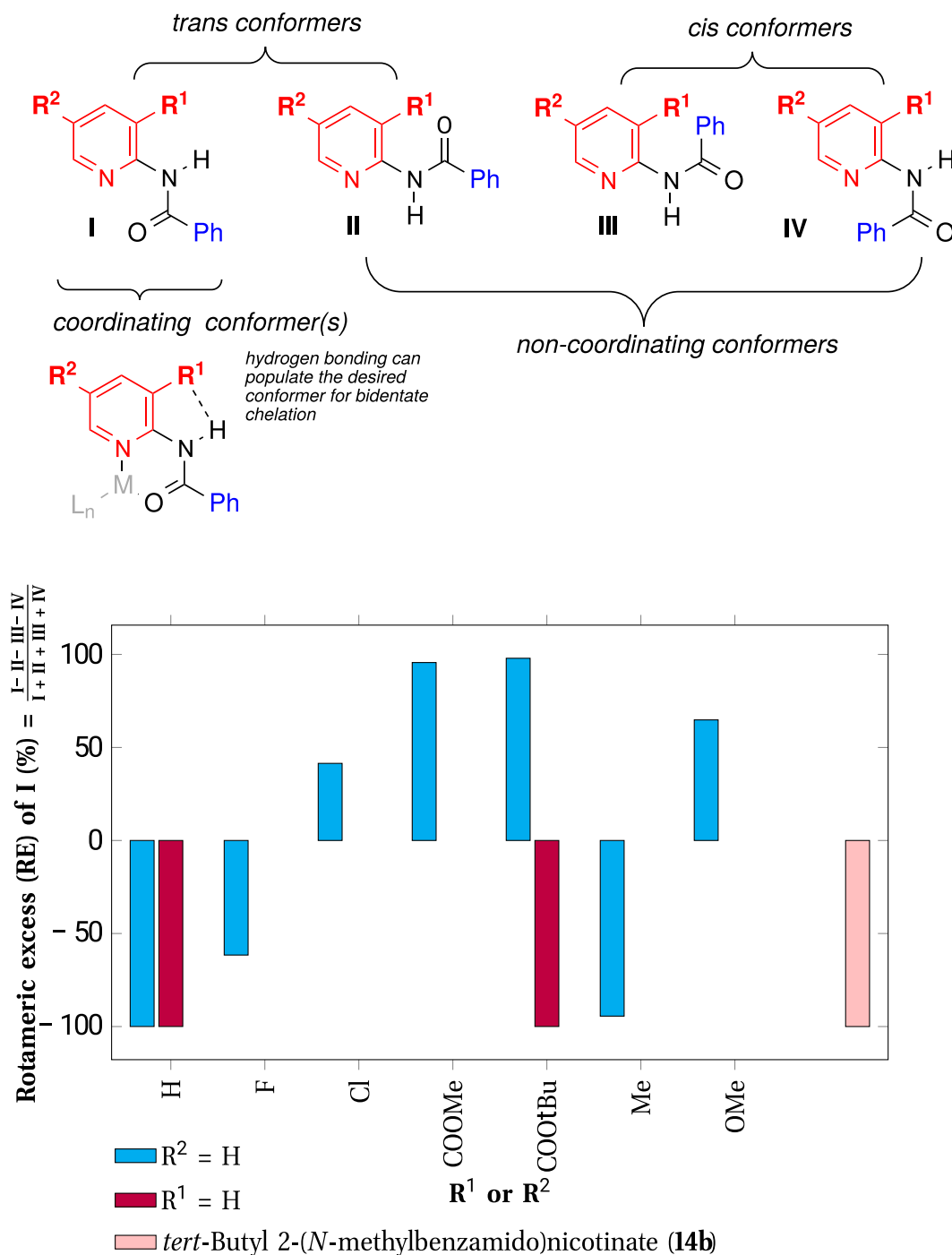
Benzamide (**1c**) equipped with a *py*-DG (**8a**) was used as an initial test substrate for the optimization of the amide cleavage. In a first step, several metal salts (Fe, Cu, Zn, Co, Mn, Ni; 10.0 mol%) were screened as potential catalysts in alcohol, used as both nucleophile and solvent, at 140 and 75 °C (Table 1, SI S.3.2). The more challenging secondary alcohol isopropanol (**2c**) was selected over a primary alcohol for the method development phase. This screening under solvolytic conditions resulted in the identification of  $\text{Zn}(\text{OAc})_2$  as the optimal catalyst for further development based on its low cost, non-toxicity and conversion. In order to further reduce the required temperature for amide cleavage and increase in conversion, the effect of substitution onto the *py*-DG was subsequently studied with both electron-withdrawing (F, Cl, COOR, CN,  $\text{CF}_3$ ) and -donating (Alkyl, Ph, OR) groups. Substitution at the C3- and C5-positions of the *py*-DG was explored since the same group at both positions has a similar electronic, but different electrostatic effect, which can be electrostatic repulsive (steric effect) or attractive (intramolecular hydrogen bond) (Figure 2, SI S.3.2.4-S.3.2.5). A C3-Cl, -OMe or -COOR-substituent gave the best results at 75 °C (Figure 2a). Of these, an ester at C3 of the *py* turned out to be the most efficient substituent, as the required temperature for isopropanolysis with these DGs could be lowered to 40 °C (Figure 2b). The suitability of the C3-Cl, -OMe or -COOR-substituted *py*-DG is in accordance with the

1 predicted population of the *trans*-conformer(s) **I** of the corresponding *N*-(pyridin-2-yl)benzamide  
 2 **8** and **13a** (Figure 1, Table S35). The exceptional performance of the alkyl nicotinate DGs at 40  
 3 °C is in accordance with the complete locking of the *N*-DG amide in its conformer **I**. The reac-  
 4 tivity difference between an ether and ester at C3 of the DG is likely also due to the electron  
 5 withdrawing effect of the ester causing a further reduction in amide resonance energy (N(n)-  
 6  $\pi^*(Ar)$  delocalization).<sup>11</sup> Resonance energy calculations support this (4.2 kcal/mol for *tert*-butyl  
 7 2-benzamidonicotinate (**13a**) versus 8.2 kcal/mol for *N*-(3-methoxypyridin-2-yl)benzamide (**8s**)) (SI  
 8 S.9.2). *tert*-Butyl and isopropyl nicotinate (*tBu/iPr nic*) performed equally well as DGs, but the  
 9 former was chosen for further studies to avoid potential transesterification with alcohol. At 40 °C,  
 10 isopropanolysis of *tert*-butyl 2-benzamidonicotinate (**13a**) with 10 mol% of Zn(OAc)<sub>2</sub> resulted in full  
 11 conversion to isopropyl benzoate (**9a**) (87% yield) and *tert*-butyl 2-aminonicotinate (**10a**) (96% yield)  
 12 in 48 h (standard conditions). The formed by-product **10a** can be easily transformed in one-step  
 13 into *tert*-butyl 2-chloronicotinate (**11a**) via diazotization using *aq.* HCl and NaNO<sub>2</sub> in the presence  
 14 of NaCl (Scheme 4, SI S.8), thus enabling recovery of the reactant required for DG-introduction  
 15 (Scheme 4).  
 16  
 17  
 18  
 19  
 20  
 21  
 22  
 23  
 24  
 25  
 26  
 27  
 28  
 29  
 30  
 31  
 32



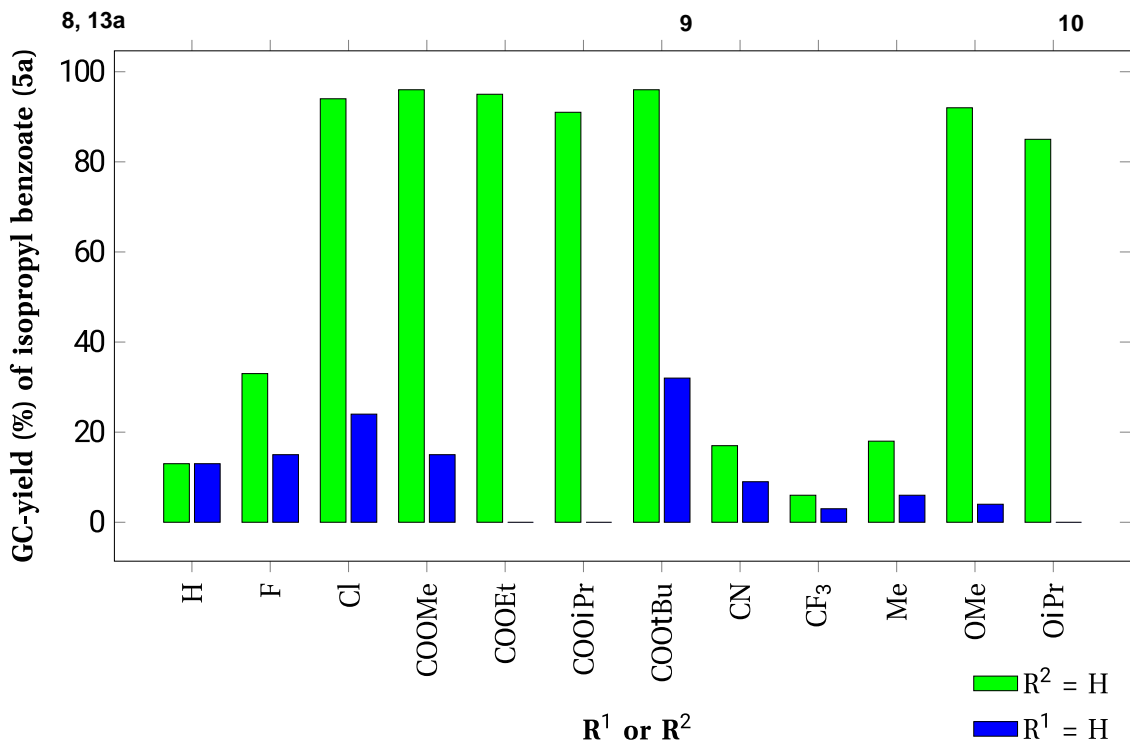
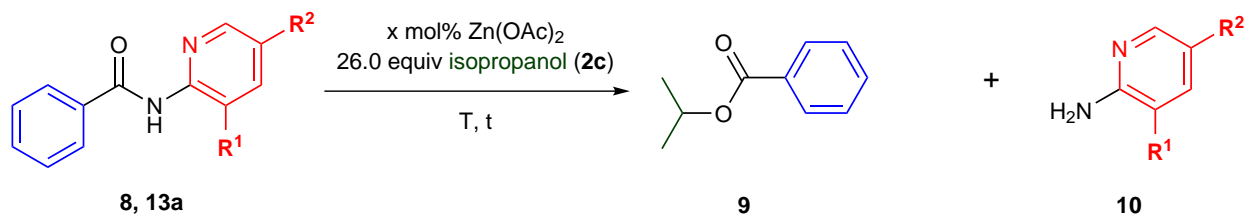
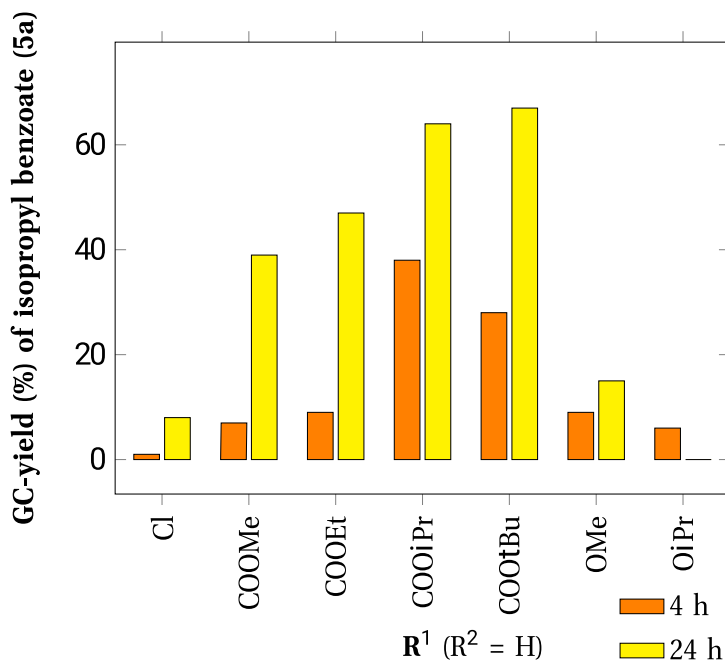
Scheme 4: Synthesis of *tert*-butyl 2-chloronicotinate (**11a**) reactant from *tert*-butyl 2-aminonicotinate (**10a**) by-product produced in the directed amide cleavage with alcohols **2**.

With the optimal DG in hand, a method to smoothly introduce *tBu nic* onto primary amides **1**, at  
 an equally mild temperature as required for the cleavage, was needed (SI S.3.1). Evaluation of the  
 Pd-catalyzed amidation of *tert*-butyl 2-chloronicotinate (**11a**) with benzamide (**1c**) led to the identifi-  
 cation of the Buchwald Pd G3 precatalyst **12a** of the ligand 1,1'-bis(dicyclohexylphosphino)ferrocene  
 (dcppf) (**7b**) as the optimal precatalyst system (Table 2).<sup>17, 18</sup> Both the use of Cs<sub>2</sub>CO<sub>3</sub> (1.2 equiv) as an  
 inorganic weak base and the renewable solvent 2-MeTHF proved to be indispensable to obtain full  
 conversion at 40 °C in 24 h with an isolated yield of 97% of *tert*-butyl 2-benzamidonicotinate (**13a**).  
 Both Cs<sub>2</sub>CO<sub>3</sub> and 2-MeTHF are recommended from a sustainability point of view.<sup>19</sup> Interestingly,



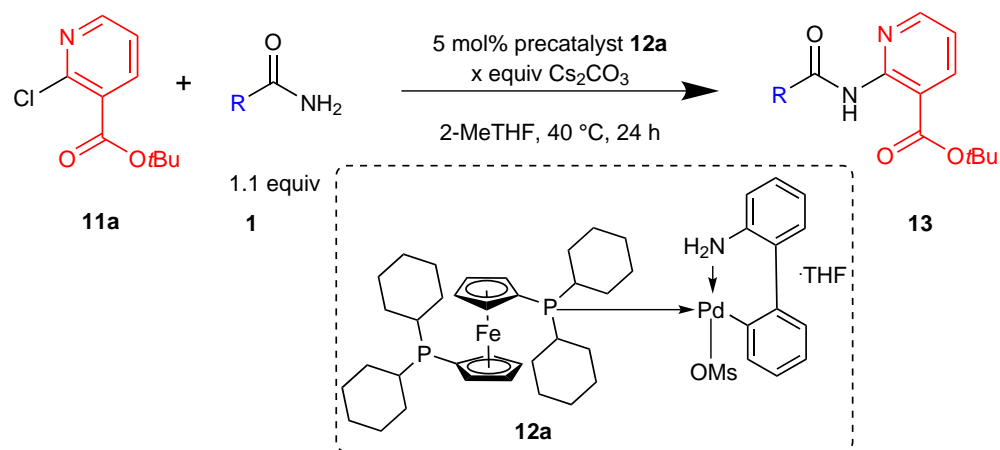
Conformational analysis of *N-py* amides via DFT-calculations at the SCRF/B3LYP/6-31G(d,p) level of theory (T = 298 K), using 'Gaussian 09' software; see Supporting Information (SI 9.1.2). The self-consistent reaction field (scrf) model was used to account for solvent-solute interactions with butyl acetate, as a model for the effect of *tert*-butyl acetate, the main solvent used for the experimental cleavage reactions. RE > 0: desired reactive conformer **I** is the major conformer.

Figure 1: Rationalization of the directing group screening via computational conformational analysis of (C3- and C5-substituted) *N*-(pyridin-2-yl)benzamides **8** and **13a**.

(a) 25 mol%  $\text{Zn}(\text{OAc})_2$ , 75 °C, 6 h.(b) 10 mol%  $\text{Zn}(\text{OAc})_2$ , 40 °C, 4 h and 24 h.Figure 2: Directing group screening in the Zn-catalyzed directed cleavage of C3- and C5-substituted *N*-(pyridin-2-yl)benzamides **8** and **13a**.

1  
2  
3 the optimal dcpf ligand **7b** identified has not been described yet as a ligand for Pd-catalyzed  
4 amidations. The applicability of the identified conditions to a variety of primary amides **1** was  
5 explored (Table 2). Sometimes further fine-tuning of the DG-introduction conditions was required  
6 (SI S.3.1.3), involving the use of more Cs<sub>2</sub>CO<sub>3</sub> (1.2-7.5 equiv), K<sub>2</sub>CO<sub>3</sub> instead of Cs<sub>2</sub>CO<sub>3</sub> and DMF  
7 as a co-solvent to allow full conversion at 40–50 °C within 24 hours. The positive effect of larger  
8 amounts of insoluble weak carbonate base on the rate of Buchwald-Hartwig reactions (base-effect)  
9 has been previously reported and rationalized by our group (SI S.3.1.2).<sup>20</sup> With these small mod-  
10 ifications, the identified protocol proved to be applicable to all types of primary amides, both  
11 (hetero)aromatic and (a)cyclic aliphatic ones. This also includes very challenging representatives  
12 such as Boc-(AA)<sub>n</sub>-NH<sub>2</sub> derivatives (AA = amino acid, n = 1-3).<sup>21</sup> Interestingly, primary amides  
13 **1** can be selectively *N*-arylated in the presence of secondary amides as exemplified by Boc-L-  
14 Pro-L-Phe-NH<sub>2</sub> (**1a**) and Boc-L-Pro-L-Leu-Gly-NH<sub>2</sub> (**1p**).<sup>17b,c</sup> Chemoselectivity is also possible versus  
15 other functionalities as illustrated by atenolol (**1q**), an API-carboxamide containing an unprotected  
16 hydroxyl group and a secondary amine. Considering the weakly nucleophilic nature of amides  
17 classical reaction with electrophiles via S<sub>N</sub>AE, e.g. bacylation with Boc<sub>2</sub>O, generally do not allow  
18 such chemoselectivity and reaction will (additionally) occur at the more nucleophilic sites.<sup>22</sup> In  
19 all cases, full conversion and good to excellent yields of *tert*-butyl 2-amidonicotines **13** were  
20 obtained. Pd(OAc)<sub>2</sub> in combination with Xantphos ligand in dioxane with K<sub>2</sub>CO<sub>3</sub> as base could  
21 also be used to introduce the directing group, provided a higher reaction temperature is applied  
22 (Table 2).<sup>17d</sup> These synthesized *tert*-butyl 2-amidonicotines **13** allowed solvolytic cleavage with  
23 primary and secondary (un)branched aliphatic alcohols **2** under the developed standard reaction  
24 conditions (*vide supra*) (SI S.3.4).  
25  
26  
27  
28  
29  
30  
31  
32  
33  
34  
35  
36  
37  
38  
39  
40  
41  
42  
43  
44  
45  
46  
47  
48  
49  
50  
51  
52  
53  
54  
55  
56  
57  
58  
59  
60

Table 2: *tert*-Butyl nicotinate introduction on primary amides **1** via Pd-catalyzed amidation of *tert*-butyl 2-chloronicotinate (**11a**). Reaction times were not minimized.



Entry	RCONH <sub>2</sub>	<b>1</b>	<i>x</i>	Yield <b>13</b> <sup>1</sup>
1		<b>1c</b>	1.2	<b>13a</b> , 97% (99%) 92% <sup>2</sup>
2		<b>1d</b>	1.2	<b>13b</b> , 63% (92%)
3		<b>1e</b>	1.2	<b>13c</b> , 78% (92%)
4		<b>1f</b>	7.5	<b>13d</b> , 99% (quant.) 78% <sup>2</sup>
5		<b>1g</b>	1.2	<b>13e</b> , 92% (93%)
6		<b>1h</b>	1.2	<b>13f</b> , 75% (98%)
7		<b>1i</b>	1.2	<b>13g</b> , 86% (quant.)
8		<b>1j</b>	5	<b>13h</b> , 83% (quant.)
9		<b>1k</b>	1.2	<b>13i</b> , 59% (94%)

10	Boc-Gly-NH <sub>2</sub>	<b>1l</b>	1.2	<b>13j</b> , 83% (quant.)
11	Boc-L-Pro-NH <sub>2</sub>	<b>1m</b>	1.2	<b>13k</b> , 80% <sup>2</sup> (95%) 91% <sup>2,3</sup>
12	Boc-L-Val-NH <sub>2</sub>	<b>1n</b>	2	<b>13l</b> , 98% <sup>2</sup> (92%) 94% <sup>3,4</sup>
13	Boc- $\beta$ -Ala-NH <sub>2</sub>	<b>1o</b>	2	<b>13m</b> , 99% (quant.)
14	Boc-D-Phe-NH <sub>2</sub>	<b>1b</b>	7.5	<b>13n</b> , 92% (93%) <sup>5</sup>
15	Boc-L-Phe-NH <sub>2</sub>	<b>1aj</b>	7.5	<b>13ak</b> , 93% (96%) <sup>5</sup>
16	Boc-L-Pro-L-Phe-NH <sub>2</sub>	<b>1a</b>	2	<b>13o</b> , 93% (78%) <sup>6,7</sup>
17	Boc-L-Pro-L-Leu-Gly-NH <sub>2</sub>	<b>1p</b>	7.5	<b>13p</b> , 99% (quant.) <sup>7,8</sup>
18	Atenolol	<b>1q</b>	2.5	<b>13q</b> — (95%) <sup>9</sup>

<sup>1</sup> 5 mol% precatalyst **12a**, x equiv. Cs<sub>2</sub>CO<sub>3</sub>, 2-MeTMF, 40 °C, 24 h unless mentioned otherwise. NMR-yield with TMB as internal standard between brackets; <sup>2</sup> e.e. > 98%; <sup>3</sup> 5 mol% Pd(OAc)<sub>2</sub>, 10 mol% Xantphos, 4 equiv. K<sub>2</sub>CO<sub>3</sub>, dioxane, 90 °C; <sup>4</sup> e.e. 93%; <sup>5</sup> dioxane, 7.5 equiv. K<sub>2</sub>CO<sub>3</sub>, 50 °C, 30 h; <sup>6</sup> 2-MeTHF:DMF 1:1; <sup>7</sup> d.e. > 99%; <sup>8</sup> 10 mol% **12a**; <sup>9</sup> 10 mol% **12a**, oven-dried Cs<sub>2</sub>CO<sub>3</sub>.

The formed by-product **10a** can be easily transformed in one-step into *tert*-butyl 2-chloronicotinate (**11a**) via diazotization using *aq.* HCl and NaNO<sub>2</sub> in the presence of NaCl (Scheme 4, SI S.8), thus enabling recovery of the reactant required for DG-introduction (Scheme 4).

Next the suitability for non-solvolytic *t*Bu *nic*-directed cleavage was studied. Online-IR reaction monitoring experiments of the Zn-catalyzed directed cleavage of *tert*-butyl 2-benzamidonicotinate **13a** with different alcohols **2** (5.0 equiv) were subsequently performed in order to evaluate whether alcoholysis under non-solvolytic conditions was also possible. *t*BuOAc was selected as the solvent based on its green properties (Figure 3, SI S.7).<sup>19</sup> Kinetic analysis showed that primary alcohols give substantially faster reactions than secondary ones, but both are suited for non-solvolytic use at low reaction temperatures. Full cleavage of **13a** with the use of primary alcohols such as MeOH (**2d**) (2.50 equiv in *t*BuOAc) takes only 30 minutes at 60 °C (Figure 3). To establish the same result at 40 °C, 10.0 equiv of MeOH (**2d**) are necessary (Figure 3). On the other hand, when

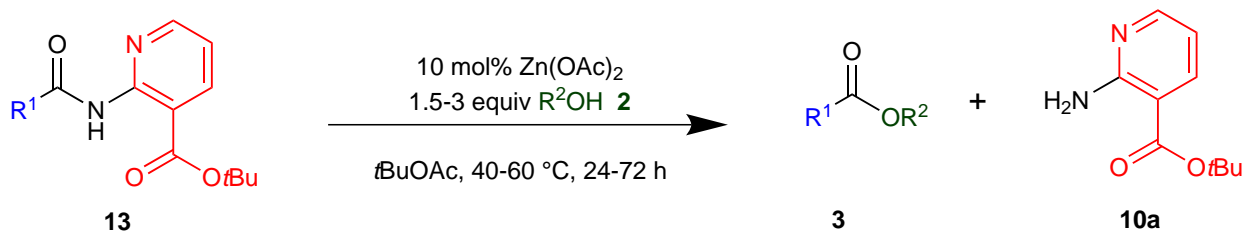


1  
2 using 1.5 equiv of MeOH (**2d**) in *t*BuOAc, full cleavage of substrate **13a** is also possible at room  
3 temperature in one day. To the best of our knowledge, such performance is unprecedented in  
4 current literature. The hitherto mildest known non-enzymatic cleavage of benzamide (**1c**) with the  
5 use of a stoichiometric amount of MeOH (**2d**) under neutral conditions without first pre-activating  
6 benzamide (**1c**) to a non-carboxamide containing intermediate, requires 165 °C for 22 h (CeO<sub>2</sub>-  
7 catalysis, 1.0 equiv MeOH (**2d**) in mesitylene).<sup>4</sup>

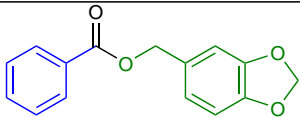
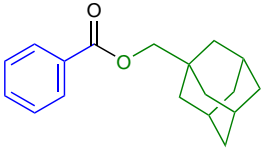
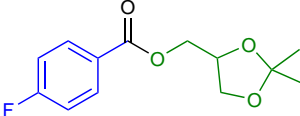
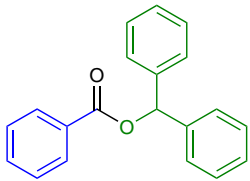
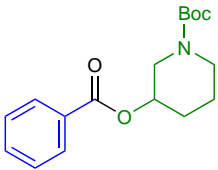
8  
9 Based on our screening of non-solvolytic amide cleavage (SI S.3.6), 3.0 equiv of alcohol **2** and 10  
10 mol% Zn(OAc)<sub>2</sub>-catalyst were selected for the investigation of the non-solvolytic alcohol scope in  
11 the Zn-catalyzed *tert*-butyl nicotinate directed amide cleavage of **13**, using *t*BuOAc as a solvent  
12 (Table 3-5). Interestingly, alcohols that are solids, which cannot be used solvolytically at 40 °C, and  
13 more complex or expensive ones proved to be suitable nucleophiles for the non-solvolytic amide  
14 cleavage reaction. The use of primary and secondary acyclic aliphatic alcohols for the cleavage  
15 of (a)cyclic aliphatic and aromatic amides led to good to excellent isolated yields of the esters  
16 **3d-3o** (Table 3). Structurally more complex alcohols were successfully applied, as exemplified by  
17 the use of the sugars diaceton- $\alpha$ -D-galactopyranose (**2a**) and diaceton- $\alpha$ -D-glucose (**2k**) (esters **3p-**  
18 **3q**), sterols such as cholesterol (**2b**) (esters **3r-3s**) and dehydroepiandrosterone (**2j**) (ester **3t**) and  
19 naturally occurring alcohols such as L-menthol (**2l**) (esters **3u-3v**) and cinnamyl alcohol (**2n**) (ester  
20 **3x**) (Table 4). Moreover, amino acid-derived alcohols such as aminoalcohol **2o** derived from Boc-L-  
21 Phe-OH (ester **3y**) and Cbz-L-Ser-OMe (**2p**) (ester **3z**) are also suitable nucleophiles (Table 5). Both  
22 simple and more complex alcohols could also be combined with amino acid- and peptidic-derived  
23 *t*Bu *nic* amides **13** (esters **3w** (Table 4), **3aa, 3ab, 3b, 3ac, 3ad, 3ae, 3af, 3a, 3ag, 3ah, 3ai** (Table  
24 5)). The efficient synthesis of different cholesteryl esters **3b, 3ac, 3ad, 3ae, 3af**, glycopeptides **3a,**  
25 **3ag, 3ah** and other chimeric dipeptides **3ai** in a racemization- and epimerization-free manner  
26 illustrates the power of the developed synthetic methodology. As indicated in the tables, depending  
27 on the complexity of both amide and nucleophile slightly modified reaction conditions involving  
28 higher catalyst loading, (15 or 20 mol%), higher reaction temperature (40 to 60 °C), longer reaction  
29 time (24 to 72 h) or solvent change due to solubility problems (**3r-3t, 3b, 3ac, 3ad, 3ae, 3af**) were  
30 sometimes required to achieve full conversion. Longer reaction times could easily be shortened  
31 if higher temperatures (80 °C) were applied, as exemplified by the synthesis of **3d, 3h, 3x** (Tables  
32  
33  
34  
35  
36  
37  
38  
39  
40  
41  
42  
43  
44  
45  
46  
47  
48  
49  
50  
51  
52  
53  
54  
55  
56  
57  
58  
59  
60

1  
2 3 and 4). We always selected the lowest temperature possible to showcase the mildness of the  
3 developed protocol. Sterically hindered amides, such as (aza)cycloalkanecarboxamides (R-CONH-  
4 *t*Bu *nic*; R = cyclohexyl (**13i**); Boc-L-Pro-NH-*t*Bu *nic* (**13k**)) are more difficult to cleave than other  
5 aliphatic amide substrates (Tables 3 and 5, e.g. **3d**, **3e**, **3aa** versus Table 3, **3f**, **3g**). The same  
6 observation stands for the acyclic sterically hindered *N-t*Bu *nic* pivalamide (**13h**) (**3s**) (Table 4).  
7 Note that **3a** and **3b** which cannot be synthesized from the corresponding primary amide using  
8 Lewis acid catalysis (Scheme 1), could be obtained under mild conditions and in good yield using  
9 our two-step synthetic methodology.  
10  
11  
12  
13  
14  
15  
16  
17  
18  
19  
20  
21  
22  
23  
24  
25  
26  
27  
28  
29  
30  
31  
32  
33  
34  
35  
36  
37  
38  
39  
40  
41  
42  
43  
44  
45  
46  
47  
48  
49  
50  
51  
52  
53  
54  
55  
56  
57  
58  
59  
60

Table 3: Standard alcohol scope in the non-solvolytic Zn-catalyzed *tert*-butyl nicotinate directed amide cleavage. Reaction times used for full conversion were not minimized and reactions were screened every 12 h. Lowest possible temperature was selected.



Entry	Substrate <b>13</b>	Ester <b>3</b>	Yield <sup>a,b</sup> (%)
1	<b>13i</b>		<b>3d</b> 66 (97) (89) <sup>c,d</sup>
2	<b>13i</b>		<b>3e</b> 66 <sup>e,f</sup>
3	<b>13f</b>		<b>3f</b> 60 <sup>g</sup>
4	<b>13g</b>		<b>3g</b> 46 <sup>g</sup>
5	<b>13a</b>		<b>3h</b> quant. <sup>h</sup> (quant.) <sup>c,i</sup> (65) <sup>h,j</sup>
6	<b>13a</b>		<b>3i</b> 63 <sup>h</sup>
7	<b>13a</b>		<b>3j</b> 70 <sup>h</sup>

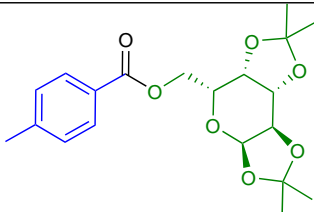
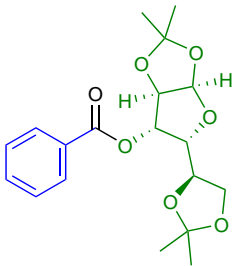
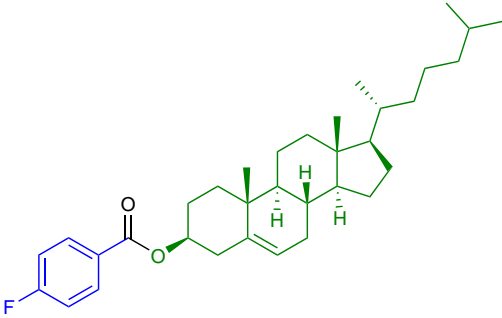
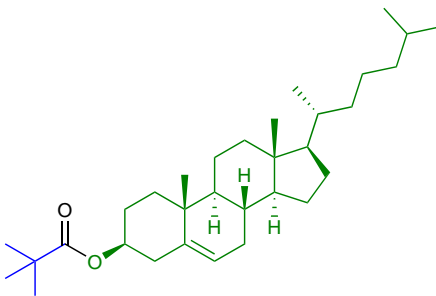
Entry	Substrate <b>13</b>	Ester <b>3</b>	Yield <sup>a,b</sup> (%)
8	<b>13a</b>		<b>3k</b> 52
9	<b>13a</b>		<b>3l</b> 55
10	<b>13b</b>		<b>3m</b> 78
11	<b>13a</b>		<b>3n</b> 56
12	<b>13a</b>		<b>3o</b> 65

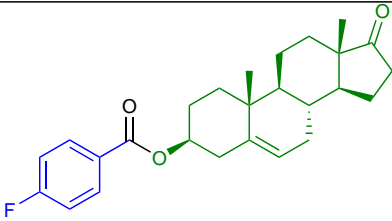
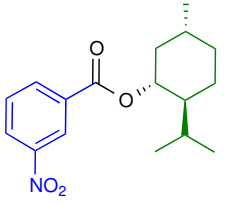
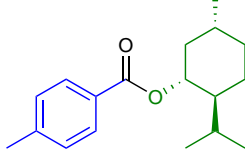
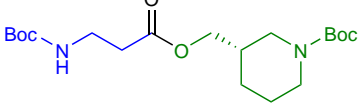
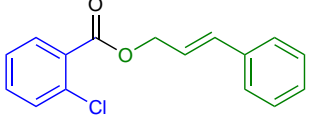
<sup>a</sup> 10 mol% Zn(OAc)<sub>2</sub>, 3 equiv R<sup>2</sup>OH **2**, *t*BuOAc, 40 °C, 48 h unless mentioned otherwise. <sup>b</sup> Isolated yield. NMR-yield with 1,3,5-trimethoxybenzene as internal standard between brackets. <sup>c</sup> 80 °C. <sup>d</sup> 36 h. <sup>e</sup> 60 °C. <sup>f</sup> 72 h. <sup>g</sup> 1.5 equiv R<sup>2</sup>OH **2**. <sup>h</sup> 24 h. <sup>i</sup> 4 h. <sup>j</sup> Reaction based on crude **13**, yield over two steps.

Table 4: Complex alcohol scope in the non-solvolytic Zn-catalyzed *tert*-butyl nicotinate directed amide cleavage. Reaction times used for full conversion were not minimized and reactions were screened every 12 h. Lowest possible temperature was selected.

Reaction scheme showing the Zn-catalyzed *tert*-butyl nicotinate directed amide cleavage:

Substrate **13** (with  $R^1$  and  $OR^2$  groups) reacts with 10-20 mol%  $Zn(OAc)_2$  and 3 equiv  $R^2OH$  **2** in  $tBuOAc$  or 2-MeTHF at 50 °C for 24-72 h to yield Ester **3** and Nicotinic acid derivative **10a**.

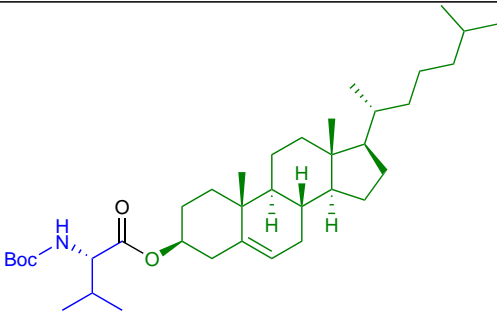
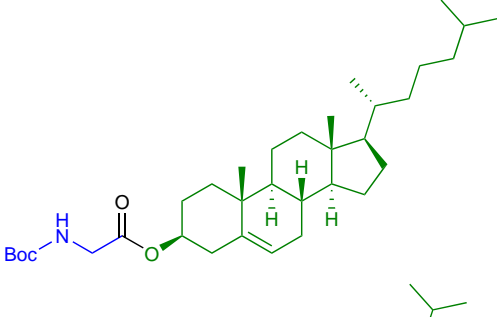
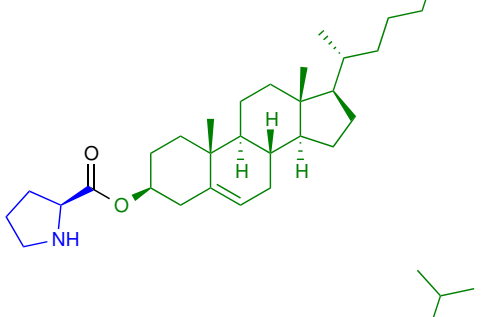
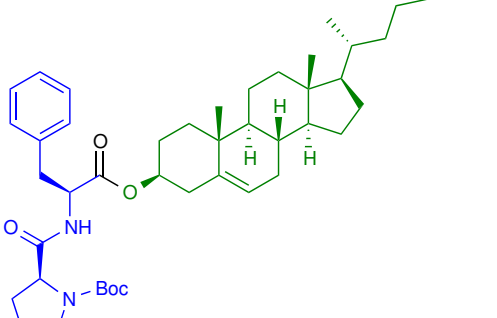
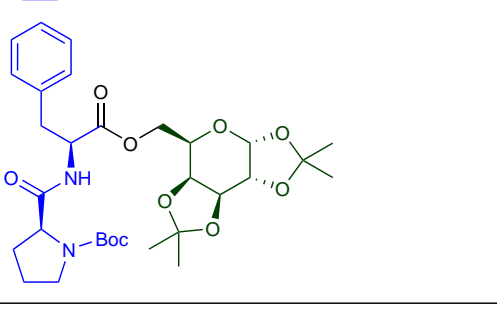
Entry	Substrate <b>13</b>	Ester <b>3</b>	Yield <sup>a,b</sup> (%)
1	<b>13e</b>		<b>3p</b> 74 <sup>c</sup>
2	<b>13a</b>		<b>3q</b> 75 <sup>c,d</sup>
3	<b>13b</b>		<b>3r</b> 59 <sup>e,f</sup>
4	<b>13h</b>		<b>3s</b> 60 <sup>f,g,h</sup>

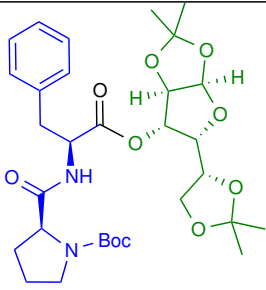
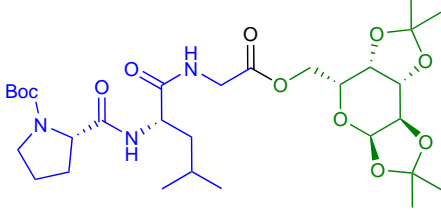
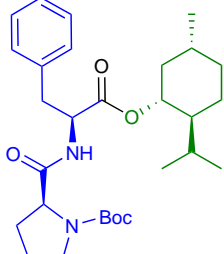
Entry	Substrate <b>13</b>	Ester <b>3</b>	Yield <sup>a,b</sup> (%)
5	<b>13b</b>		<b>3t</b> 61 <sup>d,f</sup>
6	<b>13d</b>		<b>3u</b> 86 <sup>c</sup>
7	<b>13e</b>		<b>3v</b> quant. <sup>c</sup>
8	<b>13m</b>		<b>3w</b> 86 <sup>e</sup>
9	<b>13c</b>		<b>3x</b> 86 <sup>c</sup> (91) <sup>i,j</sup>

<sup>a</sup> 10 mol% Zn(OAc)<sub>2</sub>, 3 equiv R<sup>2</sup>OH **2**, *t*BuOAc, 50°C, 48 h unless mentioned otherwise. <sup>b</sup> Isolated yield. NMR-yield with 1,3,5-trimethoxybenzene as internal standard. <sup>c</sup> 20 mol% Zn(OAc)<sub>2</sub>. <sup>d</sup> 72 h. <sup>e</sup> 24 h. <sup>f</sup> 2-MeTHF. <sup>g</sup> 25 mol% Zn(OAc)<sub>2</sub>, 60 °C. <sup>h</sup> 3 d. 87% NMR-based conversion. <sup>i</sup> 80°C. <sup>j</sup> 18 h.

Table 5: Amino acid and peptide derived amide and alcohol scope in the non-solvolytic Zn-catalyzed *tert*-butyl nicotinate directed amide cleavage. Reaction times used for full conversion were not minimized and reactions were screened every 12 h. Lowest possible temperature was selected.

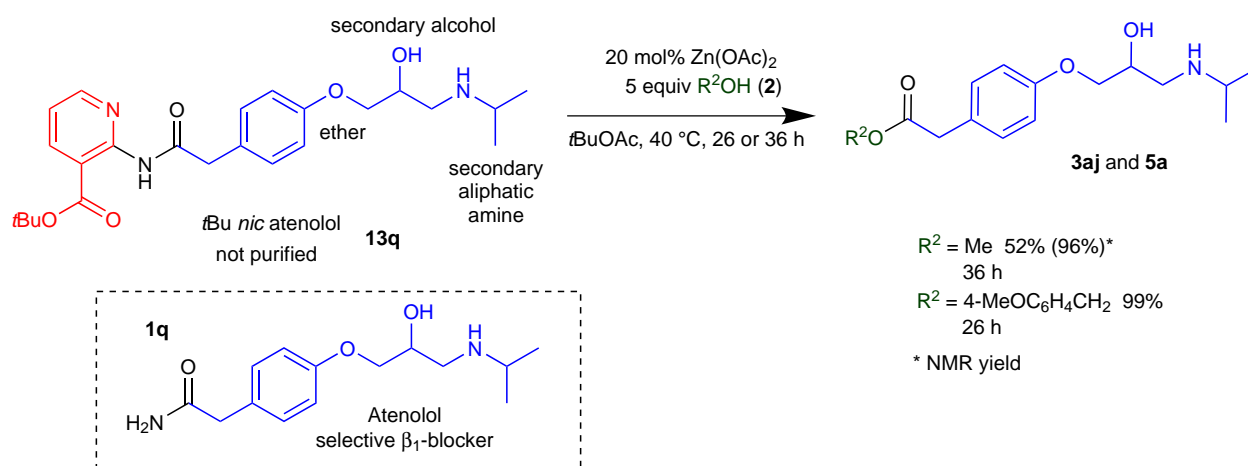
Entry	Substrate <b>13</b>	Ester <b>3</b>	Yield <sup>a,b</sup> (%)
1	<b>13a</b>		<b>3y</b> quant.
2	<b>13a</b>		<b>3z</b> 18 <sup>c</sup>
3	<b>13k</b>		<b>3aa</b> 85 <sup>d</sup>
4	<b>13j</b>		<b>3ab</b> 85 <sup>e</sup>
5	<b>13n</b>		<b>3b</b> 93 <sup>f,g,h</sup>

Entry	Substrate <b>13</b>	Ester <b>3</b>	Yield <sup>a,b</sup> (%)
6	<b>13l</b>		<b>3ac</b> 59 <sup>g,h</sup>
7	<b>13j</b>		<b>3ad</b> 82 <sup>g,h,i</sup>
8	<b>13k</b>		<b>3ae</b> 52 <sup>d,e,f,g,h</sup>
9	<b>13o</b>		<b>3af</b> 60 <sup>g,h,i</sup>
10	<b>13o</b>		<b>3a</b> 82 <sup>g,i</sup>

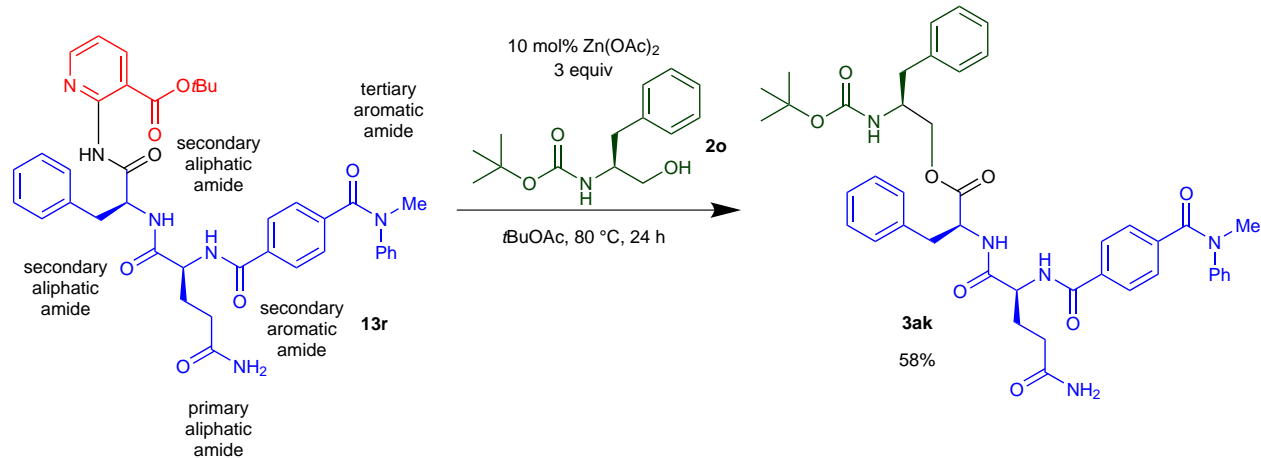
Entry	Substrate <b>13</b>	Ester <b>3</b>	Yield <sup>a,b</sup> (%)
11	<b>13o</b>		<b>3ag</b> 52 <sup>d,f,g</sup>
12	<b>13p</b>		<b>3ah</b> 69 <sup>f,g</sup>
13	<b>13o</b>		<b>3ai</b> 59 <sup>d,i,j</sup>

<sup>a</sup> 10 mol% Zn(OAc)<sub>2</sub>, 3 equiv R<sup>2</sup>OH **2**, *t*BuOAc, 40 °C, 48 h unless mentioned otherwise. <sup>b</sup> Isolated yield. NMR-yield with 1,3,5-trimethoxybenzene as internal standard between brackets. <sup>c</sup> Low yield due to difficult isolation. <sup>d</sup> 72 h. <sup>e</sup> Boc-deprotection on silica gel during purification. <sup>f</sup> 20 mol% Zn(OAc)<sub>2</sub>. <sup>g</sup> 50 °C. <sup>h</sup> 2-MeTHF. <sup>i</sup> 15 mol% Zn(OAc)<sub>2</sub>. <sup>j</sup> 60 °C.

Next we investigated chemoselectivity with respect to competitive nucleophiles and other amides in **13** (Scheme 5). For competitive nucleophilic centers we selected atenolol (**1q**). This API is a challenging substrate as it features an unprotected secondary alcohol and a secondary acyclic amine in its structure. Based on the limited quantities generally available for APIs, we preferred to evaluate a strategy without intermediate purification after DG-introduction. On crude *N-t*Bu *nic* atenolol (**13q**), smooth cleavage was observed with methanol (**2d**) or 4-methoxybenzyl alcohol (**2q**) as model alcohols (**5a**, **3aj**). Interestingly, no products resulting from intermolecular reaction of the alcohol or amine in the back bone were observed. Additionally, this strategy without purification of the intermediate seems to be generally applicable, as exemplified by the scope example **3h** (Table 3). To show chemoselectivity in amide type we selected peptidic substrate **13r** (Scheme



29 (a) Application of the cleavage methodology on the API atenolol (**1q**). See Table 2, Entry 18 for synthesis of  
30 crude **13q**.



46 (b) Application of the cleavage methodology on oligoamide containing substrate **13r**. For the synthesis of  
47 **13r**, see SI S.6.9.

50  
51  
52  
53  
54  
55  
56  
57  
58  
59  
60

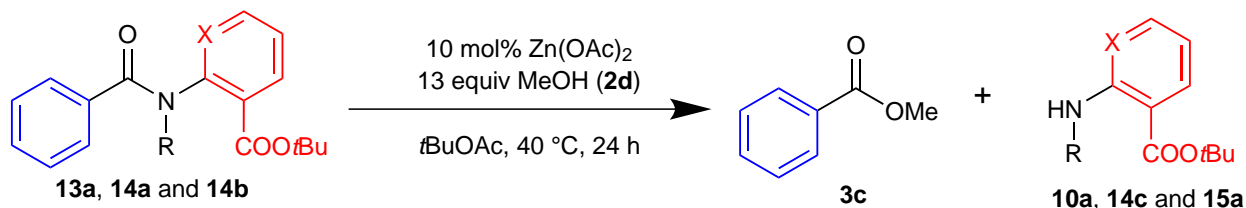
Scheme 5: Evaluation of amide chemoselectivity.

1  
2  
3 5). This structure features 5 electronically and sterically different amides (primary, secondary and  
4 tertiary amides, derived from aromatic and aliphatic carboxylic acids, both *N*-alkyl and *N*-aryl).  
5 Applying our method on **13r** with phenylalanol (**2o**) yielded the corresponding ester **3ak** in 58%  
6 yield. No other amides besides the *t*Bu *nic* activated one cleaved under these reaction conditions,  
7 exemplifying the potential applicability of our approach in organic synthesis. Important to note is  
8 that also the tertiary *N*-methyl-*N*-phenylbenzamide, which is known to undergo alcoholysis under  
9 Ni-catalysis,<sup>9a</sup> does not cleave. In fact, an aliphatic amide selectively cleaves in the presence  
10 of aromatic amides. This is against expectations based on the electrophilicity of the carbonyl  
11 moieties. The synthesis of **3ak** is a good example of the use of *N*-*t*Bu *nic* amides **13** in organic  
12 synthesis as the substrate **13r** is built up from Boc-L-Phe-NH-*t*Bu (**13ak**) *nic* via classical amide  
13 coupling reactions (Boc-deprotection: HCl in 1,4-dioxane; Amide formation: EDC.HCl, NEt<sub>3</sub>, HOBT,  
14 CH<sub>2</sub>Cl<sub>2</sub>; SI S.6.9). This illustrates the stability of *N*-*t*Bu *nic* amides **13** in the absence of zinc  
15 catalyst and nucleophile.  
16  
17  
18  
19  
20  
21  
22  
23  
24  
25  
26  
27

28  
29 To rationalize the parameters contributing to the lowering of the activation energy for directed  
30 amide alcoholysis, some specific experiments with MeOH (**2d**) were performed (SI S.9.3). The  
31 developed amide cleavage reaction is a catalytic reaction as in the absence of a metal catalyst,  
32 neither benzamide **8a** or **13a**, featuring respectively a *py*- and *t*Bu *nic*-DG, can be cleaved in  
33 the presence of an alcohol, even at 140 °C. When comparing the results obtained with the C3-  
34 and C5-substituted *py*-DGs on benzamide at the same reaction temperature (*vide supra*) and  
35 considering a chemoselective cleavage of **13r** (Scheme 5), the increased electrophilicity of the  
36 amide carbonyl through resonance cannot solely explain the observed increased reactivity of **13a**  
37 under Zn-catalysis (Figure 2). When removing the intramolecular hydrogen bond capacity of **13a**  
38 by *N*-methylation, no methanolysis was observed at 40 °C (Table 6, Entry 3), proving its potential  
39 role. *N*-methylation also results in *trans* to *cis* isomerization of the amide bond, likely also  
40 contributing to switching off the reactivity of **14b** (Supporting Table S35). Strong intramolecular  
41 hydrogen bonding in all alkyl 2-benzamidonicotines was confirmed via determination of the  
42  $A_{NMR}$ -parameter (<sup>1</sup>H-NMR analysis)<sup>23</sup> and charge density (*ab initio* calculations)<sup>24</sup> (SI S.9.4). A  
43 C3-ester substituent results in the strongest hydrogen bond, followed by a methoxy and chlorine  
44 substituent, which form weaker hydrogen bonds with the amide proton. Only C3-fluorine does not  
45  
46  
47  
48  
49  
50  
51  
52  
53  
54  
55  
56  
57  
58  
59  
60

show the presence of a hydrogen bond, which is in line with its very poor reactivity at 75 °C (Figure 2a). The reactivity difference between different substituents at C3 does not only involve a hydrogen bonding strength element. Additionally, the electron withdrawing character of substituents will cause a further reduction in amide resonance energy (N(n)- $\pi^*(Ar)$ ).<sup>11</sup> The requirement of bidentate chelation is clearly seen by using *tert*-butyl benzoate (Table 6, Entry 2) as DG, since *tert*-butyl 2-benzamidobenzoate (**14a**), lacking the azine nitrogen, does not undergo any alcoholysis at 40 °C. *N*-Phenylbenzamide (**14d**), missing both the nitrogen for bidentate coordination with Zn and a C3-HBA did not undergo alcoholysis, even at 140 °C. The amide activating effect of bidentate chelation is also reflected when comparing with the state-of-the-art classical reaction conditions for amide cleavage. After all, *N*-(hetero)arylamide cleavage normally requires an excess of a strong acid or base to allow alcoholysis.<sup>25</sup>

Table 6: Mechanistic experiments on model compounds to support the crucial factors in amide activation in the Zn-catalyzed *tert*-butyl nicotinate directed amide alcoholysis.



Entry	X	R	<b>3c</b> <sup>a</sup>	Amide <sup>b</sup>	DG-NH <sub>2</sub> <sup>b</sup>
1	N	H	quant.	<b>13a</b> , 0%	<b>10a</b> , quant.
2	CH	H	0%	<b>14a</b> , quant.	<b>15a</b> , 0%
3	N	Me	0%	<b>14b</b> , 99%	<b>14c</b> , 0%

<sup>a</sup> GC-yield with 1,3,5-trimethoxybenzene as internal standard; <sup>b</sup> NMR-yield with 1,3,5-trimethoxybenzene as internal standard.

We used density functional theory (DFT) calculations to compute the catalytic cycle for Zn-catalyzed cleavage of **13a** with methanol (**2d**); Figure 4 shows the free energy profile. Bidentate chelation of **13a** in its most stable *trans*-conformer **I** with catalyst **17** results in a more stable biomimetic precomplex **18a**. Subsequently, the hydrogen-bonded MeOH (via acetate ligand of Zn(OAc)<sub>2</sub>) can attack the amide carbonyl (**19a**), delivering intermediate **20a**. Proton transfer of the acetate proton to the exocyclic nitrogen (**22a**) allows elimination of **10a**, yielding **3c**. The importance of the ligand of the metal catalyst was also experimentally found in the initial metal catalyst screening. For example, ZnCl<sub>2</sub> was found to give lower conversion than Zn(OAc)<sub>2</sub> in

1  
2  
3 isopropanolysis at 140 °C (Table 1). The rate-determining step in the catalytic cycle of the Zn(OAc)<sub>2</sub>-  
4 catalyzed *t*Bu *nic*-directed amide cleavage of **13a** with MeOH (**2d**) is the elimination ( $\ddagger$ **22a**). When  
5  
6 computing a *py*-DG instead of a *t*Bu *nic*, the same mechanism and rate-determining step for the  
7  
8 postulated catalytic cycle is obtained. The major difference is that the precomplex **18b** is 5.3 kcal  
9  
10 mol<sup>-1</sup> less stable than **18a**. This is due to the involvement of the most stable *trans*-conformer  
11  
12 **II** of **8a**, which needs to rotate to the less stable *trans*-conformer **I** before bidentate chelation  
13  
14 becomes possible. A major kinetic difference between both pathways is therefore expected since  
15  
16 the equilibrium concentration of *trans*-conformer **I** allowing bidentate chelation, is about 12,500  
17  
18 times (weight% *trans*-**I** **13a**:**8a** = 99.517:0.008) lower for **8a** than for **13a** (Figure 1, Table S35). In  
19  
20 accordance with this, the cleavage of *N*-(pyridin-2-yl)benzamide (**8a**) under standard conditions  
21  
22 (*vide supra*; 10 mol% of Zn(OAc)<sub>2</sub>, 26.0 equiv isopropanol (**2c**), 40 °C, 48 h) does not give any  
23  
24 reaction. Under non-catalytic conditions involving 2.5 equiv Zn(OAc)<sub>2</sub> and 50 equiv of more  
25  
26 reactive MeOH (**2d**) (*which equals solvolytic alcoholysis*) at the same temperature, ester **3c** was  
27  
28 formed, but the reaction required 10 days to achieve full conversion. The cleavage reactions with  
29  
30 **13a** and **8a** are both exergonic.  
31  
32  
33  
34  
35  
36  
37  
38  
39  
40  
41  
42  
43  
44  
45  
46  
47  
48  
49  
50  
51  
52  
53  
54  
55  
56  
57  
58  
59  
60

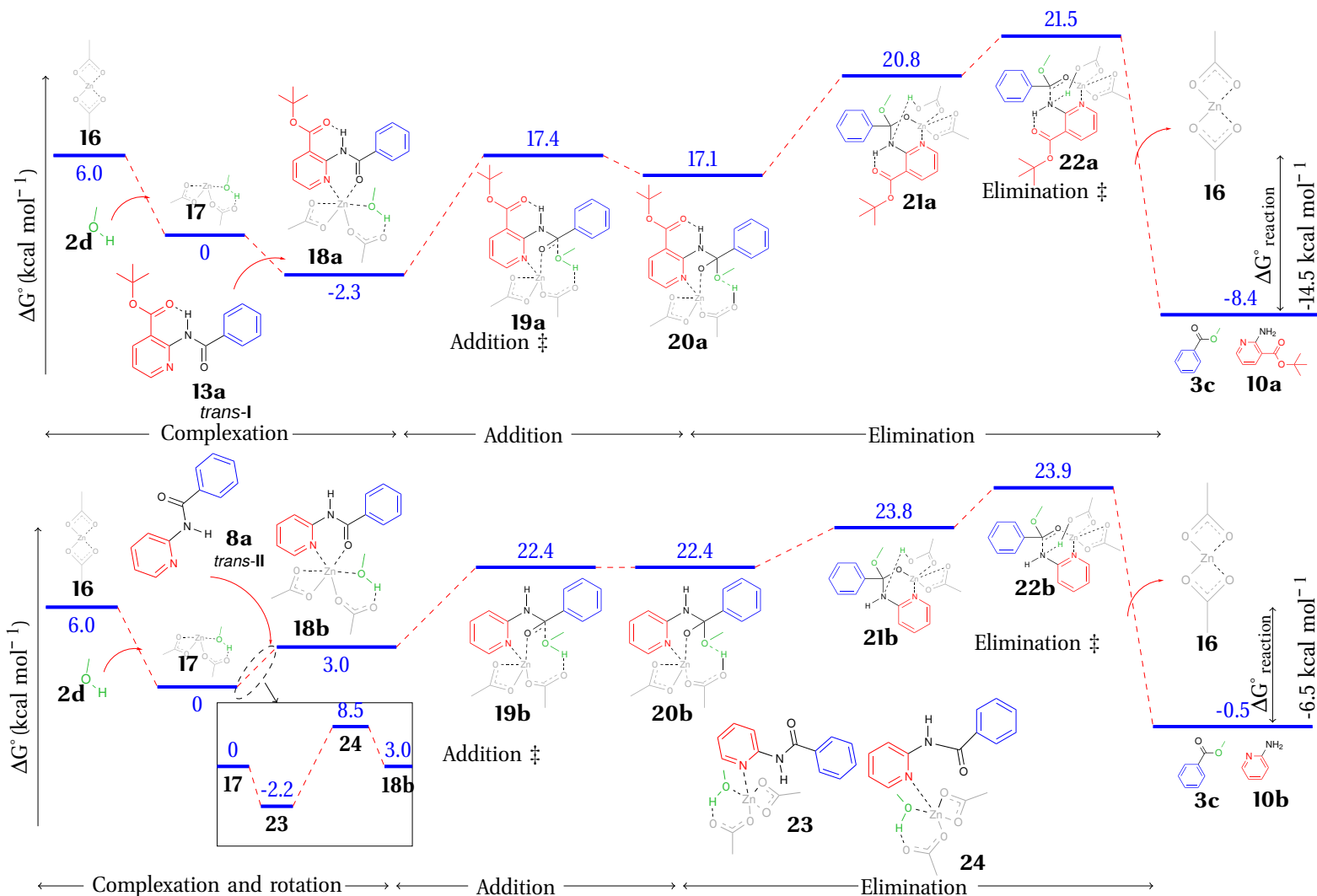
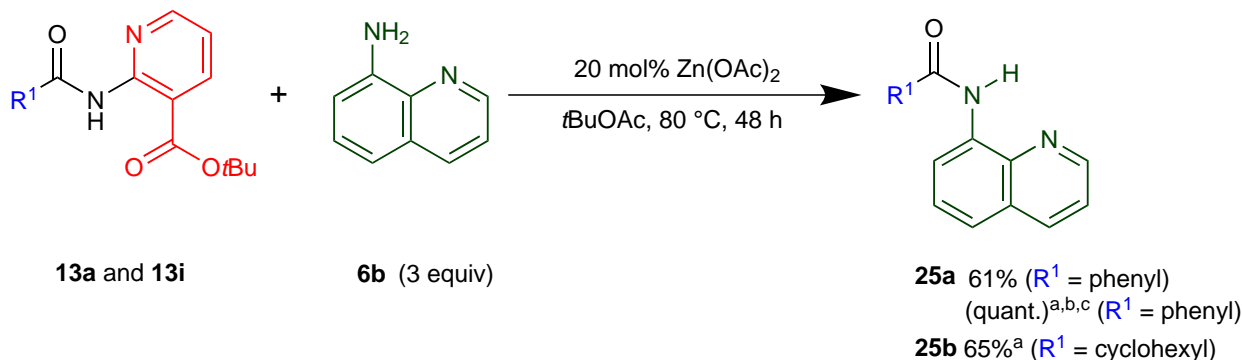


Figure 4: Computational study of the catalytic cycle of *t*Bu *nic*-directed amide cleavage of **13a** and *py*-directed amide cleavage of **8a** with MeOH (**2d**) via DFT-calculations (T = 298 K), using 'Gaussian 09' software. The self-consistent reaction field (scrf) model was used to account for solvent-solute interactions with butyl acetate, as a model for the effect of *tert*-butyl acetate, the main solvent used for the experimental cleavage reactions (figure is not on scale).

Our protocol can be considered biomimetic, as the computed reaction mechanism indeed revealed amide carbonyl activation via bidentate chelation of the catalyst with the substrate ( $C=O_{amide}-M-N_{py}$ ) and nucleophile activation via hydrogen bonding with an acetate ligand of the catalyst (Scheme 2). The rate-limiting elimination is in accordance with our experimental finding that simple carbonyl electrophilicity does not reflect the reactivity order observed.



<sup>a</sup> 100 °C, <sup>b</sup> 17 h, <sup>c</sup> NMR-yield with 1,3,5-trimethoxybenzene as internal standard.

Scheme 6: Non-solvolytic Zn-catalyzed *tert*-butyl nicotinate directed amide cleavage of **13a** and **13i** with 8-aminoquinoline (**6b**). Reaction times used for full conversion were not minimized and reactions were screened every 12 h. Lowest possible temperature was selected.

Finally, we briefly explored if other weak nucleophiles than alcohols could be used in our protocol without requiring re-optimization. Arylamines **6** have recently been used in (Ni-catalyzed) transamidation of *N*-Boc activated secondary amides,<sup>26,12c</sup> so we wondered whether our *N*-*t*Bu *nic* activated primary amides would allow Zn-catalyzed transamidation (Scheme 6). 8-Aminoquinoline (**6b**) was chosen as a model nucleophile as it is an example of a heteroaromatic amine, possessing a competitive coordination site (azine nitrogen). Moreover, in this specific case there is a chelating 1,2-diamino moiety present, making it a particularly challenging nucleophile. Not surprisingly to the best of our knowledge it has not been used as a nucleophile in metal-catalyzed transamidations. Its choice is additionally based on its widespread use as an auxiliary in transition metal-catalyzed directed C(sp<sup>2</sup>)-H and C(sp<sup>3</sup>)-H functionalization.<sup>15,27</sup> 8-Aminoquinoline (**6b**) was introduced by Daugulis in 2005,<sup>28</sup> and is typically installed in a substrate via amide bond formation with carboxylic acid delivering a bidentate directing group suitable for directed C-H functionalization. The popularity of the DG is based on the easy removability of the auxiliary by

amide hydrolysis or alcoholysis,<sup>8b,29,30</sup> *N*-*t*Bu *nic* benzamide (**13a**) was used as a model substrate. Interestingly, transamidation of **13a** with 8-aminoquinoline (**6b**) worked smoothly under the conditions optimized for alcoholysis, provided a higher catalyst loading (20 mol%) and temperature (80 °C) were applied. Also activated primary aliphatic amides, as exemplified by *N*-*t*Bu *nic* cyclohexanecarboxamide (**13i**), proved suitable substrates. As observed for alcohols **2**, a shorter reaction time is required when a higher reaction temperature is selected as illustrated for **13a**.

## Conclusions

In this work, we have developed conditions for the directed Zn-catalyzed non-solvolytic cleavage of secondary amides, through activation of the corresponding primary amides with a directing group (DG), with alcohols at 40-60 °C under neutral conditions. The Zn(OAc)<sub>2</sub> catalyst used is air stable and non toxic (E650). *tert*-Butyl nicotinate (*t*Bu *nic*) was identified as the optimal DG to overcome the inertness of the amide carbonyl. The superiority of this DG for alcoholysis can be rationalized based on hydrogen bonding between the amide proton and the ester of the DG, which results in population of the conformer needed for bidentate chelation with the Zn-catalyst (C=O<sub>amide</sub>-Zn-N<sub>py</sub>), subsequently allowing nucleophilic attack of hydrogen bond-activated alcohol on the Zn-coordinated carbonyl. Additionally the acetate ligand of Zn assists in *O*-to-*N* proton transfer. DFT calculations confirmed this and also revealed atypical rate limiting elimination. Based on these interactions, the method can be considered biomimetic with metalloproteases. The *t*Bu *nic* DG can be easily introduced onto primary amides **1** via Pd-catalyzed amidation with *tert*-butyl 2-chloronicotinate (**11a**) under mild reaction conditions provided 1,1'-bis(dicyclohexylphosphino)ferrocene is selected as ligand. This two-step cleavage protocol of primary amides, which also can be executed without isolation of the intermediate *t*Bu *nic* derived amides **13**, is compatible with both complex electrophiles (e.g. biologically active peptides) and nucleophiles (e.g. sugars and sterols) and shows excellent chemoselectivity versus other functional groups (amide, carbonate, ester, ether, acetal, alcohol, amine, alkene, halogen). This is the first general chemocatalytic method allowing cleavage of the primary amide class with non-solvolytic alcohols using a catalytic metal at low (physiological) temperature and extends the modern non-solvolytic amide cleavage toolbox beyond the known and powerful distorted tertiary amides by

1  
2  
3  
4  
5  
6  
7  
8  
9  
10  
11  
12  
13  
14  
15  
16  
17  
18  
19  
20  
21  
22  
23  
24  
25  
26  
27  
28  
29  
30  
31  
32  
33  
34  
35  
36  
37  
38  
39  
40  
41  
42  
43  
44  
45  
46  
47  
48  
49  
50  
51  
52  
53  
54  
55  
56  
57  
58  
59  
60

Boc-activation of secondary amides, towards cleavage of secondary amide substrates via *t*Bu *nic* directing group introduction on primary amides **1**. Additionally, without further elaborate reaction optimization, preliminary experiments indicate that this synthetic method can also be applied for transamidation of **13** with (hetero)arylamines **6**. Based on these preliminary results, future research will involve the use of stronger nucleophiles such as aliphatic amines **6**.

## Associated content

### Supporting Information

Supporting Information and chemical compound information are available free of charge on the ACS Publications website. Reprints and permissions information is available online. Detailed optimization data, experimental procedures, characterization data and copies of NMR spectra of all compounds.

## Author Information

### Corresponding Author

\*E-mail: Bert.Maes@uantwerpen.be

### ORCID

Bert U. W. Maes: 0000-0003-0431-7606

### Notes

The authors declare no competing financial interests.

## Acknowledgements

This work was financially supported by the University of Antwerp (BOF and IOF), the Research Foundation Flanders (FWO) (Research Projects and Scientific Research Network (WOG)) and the Hercules Foundation. Computational resources were provided by the Flemish Supercomputer Centre (VSC). The authors thank Albert Konijnenberg, Evelien Renders, Filip Desmet, Julie Charpentier,

ACS Paragon Plus Environment

1  
2 Heidi Seykens, Laurent Van Raemdonck, Norbert Hancke, Philippe Franck and Stefan Verbeeck for  
3 their (technical) support to this work.  
4  
5  
6  
7  
8

## 9 10 References

- 11  
12 1. Ruider, S.; Maulide, N. *Angew. Chem. Int. Ed.* **2015**, *54*, 13856–13858.
- 13  
14 2. Greenberg, A.; Berneman, C. M.; Liebman, J. F. *The amide linkage: structural significance in*  
15 *chemistry and biochemistry and materials science*; John Wiley and Sons, New York, 2003; p 672.
- 16  
17 3. *For some examples*; (a) Fisher, L. E.; Caroon, J. M.; Stabler, S. R.; Lundberg, S.; Zaidi, S.;  
18 Sorensen, C. M.; Sparacino, M. L.; Muchowski, J. M. *Can. J. Chem.* **1994**, *72*, 142–145; (b) Xue, C.;  
19 Luo, F.-T. *J. Chinese Chem. Soc.* **2004**, *51*, 359–362; (c) Hamilton, D.; Price, M. *J. Chem. Soc.*  
20 *D Chem. Comm.* **1969**, 414; (d) Greenlee, W.; Thorsett, E. *J. Org. Chem.* **1981**, *46*, 5351–5353;  
21 (e) Brown, R.; Bennet, A.; Slebocka-Tilk, H. *Acc. Chem. Res.* **1992**, *25*, 481–488; (f) Kita, Y.;  
22 Nishii, Y.; Onoue, A.; Mashima, K. *Adv. Synth. Catal.* **2013**, *355*, 3391–3395; (g) Nishii, Y.;  
23 Hirai, T.; Fernandez, S.; Knochel, P.; Mashima, K. *European J. Org. Chem.* **2017**, 5010–5014; (h)  
24 Atkinson, B. N.; Williams, J. M. *Tetrahedron Lett.* **2014**, *55*, 6935–6938.
- 25  
26 4. Siddiki, S. M. H.; Touchy, A. S.; Tamura, M.; Shimizu, K.-i. *RSC Adv.* **2014**, *4*, 35803–35807.
- 27  
28 5. *For reviews, accounts and perspectives*; (a) Meng, G.; Shi, S.; Szostak, M. *Synlett* **2016**, *27*, 2530–  
29 2540; (b) Dander, J. E.; Garg, N. K. *ACS Catalysis* **2017**, *7*, 1413–1423; (c) Liu, C.; Szostak, M.  
30 *Chem. Eur. J.* **2017**, *23*, 7157–7173; (d) Takise, R.; Muto, K.; Yamaguchi, J. *Chem. Soc. Rev.* **2017**,  
31 *46*, 5864–5888.
- 32  
33 6. *For some examples*; (a) Stephenson, N.; Zhu, J.; Gellman, S. H.; Stahl, S. S. *J. Am. Chem. Soc.*  
34 **2009**, *131*, 10003–10008; (b) Zhang, M.; Imm, S.; Bähn, S.; Neubert, L.; Neumann, H.; Beller, M.  
35 *Angew. Chem. Int. Ed.* **2012**, *51*, 3905–3909.
- 36  
37 7. *For examples on solvolytic amide cleavage in distorted amides*; (a) Aubé, J. *Angew. Chem. Int. Ed.*  
38 **2012**, *51*, 3063–3065; (b) Komarov, I. V.; Yanik, S.; Ishchenko, A. Y.; Davies, J. E.; Goodman, J. M.;  
39 Kirby, A. J. *J. Am. Chem. Soc.* **2015**, *137*, 926–930; (c) Yamada, S. *Angew. Chem. Int. Ed.* **1993**, *32*,  
40  
41  
42  
43  
44  
45  
46  
47  
48  
49  
50  
51  
52  
53  
54  
55  
56  
57  
58  
59  
60

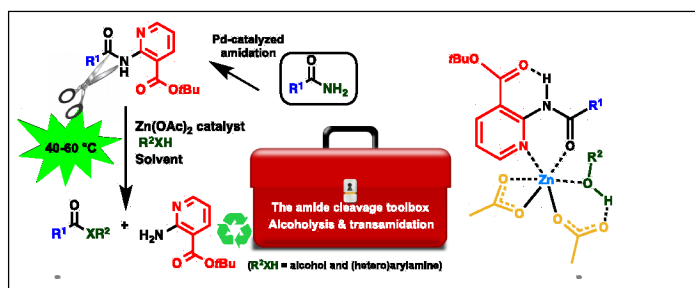
- 1  
2  
3 1083–1085; (d) Hutchby, M.; Houlden, C. E.; Haddow, M. F.; Tyler, S. N. G.; Lloyd-Jones, G. C.;  
4  
5 Booker-Milburn, K. I. *Angew. Chem. Int. Ed.* **2012**, *51*, 548–551.  
6  
7  
8 8. *For examples of leaving group activation in amides through metal chelation allowing solvolytic*  
9 *amide cleavage*; (a) Bröhmer, M. C.; Munding, S.; Bräse, S.; Bannwarth, W. *Angew. Chem. Int.*  
10 *Ed.* **2011**, *50*, 6175–6177; (b) Deguchi, T.; Xin, H.-L.; Morimoto, H.; Ohshima, T. *ACS Catal.* **2017**,  
11  
12 *7*, 3157–3161.  
13  
14  
15  
16 9. *For non-solvolytic Ni- and Co-catalyzed amide to ester transformation of N-Boc activated sec-*  
17 *ondary amide bonds*; (a) Hie, L.; Fine Nathel, N. F.; Shah, T. K.; Baker, E. L.; Hong, X.; Yang, Y.-F.;  
18  
19 Liu, P.; Houk, K. N.; Garg, N. K. *Nature* **2015**, *524*, 79–83; (b) Hie, L.; Baker, E. L.; Anthony, S. M.;  
20  
21 Desrosiers, J.-N.; Senanayake, C.; Garg, N. K. *Angew. Chem. Int. Ed.* **2016**, *55*, 15129–15132; (c)  
22  
23 Weires, N. A.; Caspi, D. D.; Garg, N. K. *ACS Catal.* **2017**, 4381–4385; (d) Bourne-Branchu, Y.;  
24  
25 Gosmini, C.; Danoun, G. *Chem. Eur. J.* **2017**, *42*, 10043–10047.  
26  
27  
28  
29 10. *For contributions describing this conjugation weakening*; (a) Szostak, R.; Shi, S.; Meng, G.;  
30  
31 Lalancette, R.; Szostak, M. *J. Org. Chem.* **2016**, *81*, 8091–8094; (b) Pace, V.; Holzer, W.; Meng, G.;  
32  
33 Shi, S.; Lalancette, R.; Szostak, R.; Szostak, M. *Chemistry â A European Journal* **2016**, *22*,  
34  
35 14494–14498.  
36  
37  
38 11. *Resonance energy in N-alkyl-N-phenylheteroareneamide is high and has recently shown*  
39 *to be significantly lowered in the corresponding (di)azine or substituted analogues (N-Me-*  
40 *N-Ph-benzamide: 13.5 kcal/mol, N-Me-N-Py-benzamide: 8.8 kcal/mol, N-Me-N-Pyr-benzamide:*  
41 *6.7 kcal/mol, N-Me-N-4-AcPh-benzamide: 11.3 kcal/mol)*; (a) Meng, G.; Lalancette, R.; Szostak, R.;  
42  
43 Szostak, M. *Org. Lett.* **2017**, *19*, 4656–4659; (b) Szostak, R.; Meng, G.; Szostak, M. *J. Org. Chem.*  
44  
45 **2017**, *82*, 6373–6378; (c) Meng, G.; Szostak, R.; Szostak, M. *Org. Lett.* **2017**, *19*, 3596–3599.  
46  
47  
48  
49  
50  
51 12. *For Ni- and Pd-catalyzed transamidation of N-Boc- or N-Ts-activated secondary amides*; (a)  
52  
53 Baker, E. L.; Yamano, M. M.; Zhou, Y.; Anthony, S. M.; Garg, N. K. *Nat. Commun.* **2016**, *7*,  
54  
55 11554; (b) Dander, J. E.; Baker, E. L.; Garg, N. K. *Chem. Sci.* **2017**, *8*, 6433–6438; (c) Meng, G.;  
56  
57 Lei, P.; Szostak, M. *Org. Lett.* **2017**, *19*, 2158–2161.  
58  
59  
60 13. *For recent examples of metal insertion in an activated secondary amide bond involving C-C and*

- 1  
2  
3 *C-B bond formation*; (a) Weires, N. A.; Baker, E. L.; Garg, N. K. *Nat. Chem.* **2016**, *8*, 75–79; (b)  
4 Meng, G.; Szostak, M. *Org. Lett.* **2016**, *18*, 796–799; (c) Meng, G.; Szostak, M. *Org. Lett.* **2015**,  
5 *17*, 4364–4367; (d) Simmons, B. J.; Weires, N. A.; Dander, J. E.; Garg, N. K. *ACS Catal.* **2016**, *6*,  
6 3176–3179; (e) Lei, P.; Meng, G.; Szostak, M. *ACS Catal.* **2017**, *7*, 1960–1965; (f) Shi, S.; Meng, G.;  
7 Szostak, M. *Angew. Chem. Int. Ed.* **2016**, *55*, 6959–6963; (g) Liu, C.; Meng, G.; Liu, Y.; Liu, R.;  
8 Lalancette, R.; Szostak, R.; Szostak, M. *Org. Lett.* **2016**, *18*, 4194–4197; (h) Hu, J.; Zhao, Y.; Liu, J.;  
9 Zhang, Y.; Shi, Z. *Angew. Chem. Int. Ed.* **2016**, *55*, 8718–8722; (i) Meng, G.; Shi, S.; Szostak, M.  
10 *ACS Catal.* **2016**, *6*, 7335–7339; (j) Shi, S.; Szostak, M. *Org. Lett.* **2016**, *18*, 5872–5875; (k) Cui, M.;  
11 Wu, H.; Jian, J.; Wang, H.; Liu, C.; Daniel, S.; Zeng, Z. *Chem. Commun.* **2016**, *52*, 12076–12079; (l)  
12 Liu, C.; Meng, G.; Szostak, M. *J. Org. Chem.* **2016**, *81*, 12023–12030; (m) Liu, Y.; Meng, G.; Liu, R.;  
13 Szostak, M. *Chem. Commun.* **2016**, *52*, 6841–6844; (n) Liu, C.; Liu, Y.; Liu, R.; Lalancette, R.;  
14 Szostak, R.; Szostak, M. *Org. Lett.* **2017**, *19*, 1434–1437; (o) Walker, J. A.; Vickerman, K. L.;  
15 Humke, J. N.; Stanley, L. M. *J. Am. Chem. Soc.* **2017**, *139*, 10228–10231.
- 16  
17  
18  
19  
20  
21  
22  
23  
24  
25  
26  
27  
28  
29  
30 14. *For examples describing metallo-exopeptidases mode of actions*; (a) Lipscomb, W. N.; Sträter, N.  
31 *Chem. Rev.* **1996**, *96*, 2375–2433; (b) Coleman, J. E. *Curr. Opin. Chem. Biol.* **1998**, *2*, 222–234; (c)  
32 Zhang, T.; Ozbil, M.; Barman, A.; Paul, T. J.; Bora, R. P.; Prabhakar, R. *Acc. Chem. Res.* **2015**, *48*,  
33 192–200.  
34  
35  
36  
37  
38  
39 15. *For some reviews on directed synthesis (C-H functionalization)*; (a) Rouquet, G.; Chatani, N.  
40 *Angew. Chem. Int. Ed.* **2013**, *52*, 11726–11743; (b) Pototschnig, G.; Maulide, N.; Schnürch, M.  
41 *Chem. - A Eur. J.* **2017**, *23*, 9206–9232; (c) Ma, W.; Gandeepan, P.; Li, J.; Ackermann, L. *Org.*  
42 *Chem. Front.* **2017**, *4*, 1435–1467; (d) Liu, J.; Chen, G.; Tan, Z. *Adv. Synth. Catal.* **2016**, *358*,  
43 1174–1194.  
44  
45  
46  
47  
48  
49  
50 16. Poupon, E.; Nay, B. In *Biomimetic organic synthesis*; Poupon, E., Nay, B., Eds.; Wiley-VCH, Verlag  
51 GmbH & Co. KGaA, Weinheim, 2011; p 976.  
52  
53  
54  
55 17. *For examples of Pd-catalyzed amidation*; (a) Huang, X.; Anderson, K. W.; Zim, D.; Jiang, L.;  
56 Klapars, A.; Buchwald, S. L. *J. Am. Chem. Soc.* **2003**, *125*, 6653–6655; (b) Ikawa, T.; Barder, T. E.;  
57 Biscoe, M. R.; Buchwald, S. L. *J. Am. Chem. Soc.* **2007**, *129*, 13001–13007; (c) Hicks, J. D.;  
58  
59  
60

- Hyde, A. M.; Cuezva, A. M.; Buchwald, S. L. *J. Am. Chem. Soc.* **2009**, *131*, 16720–16734; (d) Yin, J.; Buchwald, S. L. *J. Am. Chem. Soc.* **2002**, *124*, 6043–6048.
18. *For selected contributions on Buchwald Pd G3 precatalysts*; (a) Bruno, N. C.; Tudge, M. T.; Buchwald, S. L. *Chem. Sci.* **2013**, *4*, 916–920; (b) Bruneau, A.; Roche, M.; Alami, M.; Messaoudi, S. *ACS Catal.* **2015**, *5*, 1386–1396; (c) Ruiz-Castillo, P.; Buchwald, S. L. *Chem. Rev.* **2016**, *116*, 12564–12649; (d) Hazari, N.; Melvin, P. R.; Beromi, M. M. *Nat. Rev. Chem.* **2017**, *1*, 0025.
19. *For (green) solvent and base selection*; (a) Fine Nathel, N. F.; Kim, J.; Hie, L.; Jiang, X.; Garg, N. K. *ACS Catal.* **2014**, *4*, 3289–3293; (b) Pace, V.; Hoyos, P.; Castoldi, L.; Domínguez De María, P.; Alcántara, A. R. *ChemSusChem* **2012**, *5*, 1369–1379; (c) Henderson, R. K.; Hill, A. P.; Redman, A. M.; Sneddon, H. F. *Green Chem.* **2015**, *17*, 945–949; (d) Prat, D.; Wells, A.; Hayler, J.; Sneddon, H.; McElroy, C. R.; Abou-Shehada, S.; Dunn, P. J. *Green Chem.* **2016**, *18*, 288–296; (e) Henderson, R. K.; Jiménez-González, C.; Constable, D. J. C.; Alston, S. R.; Inglis, G. G. A.; Fisher, G.; Sherwood, J.; Binks, S. P.; Curzons, A. D. *Green Chem.* **2011**, *13*, 854–862; (f) Jiménez-Gonzalez, C.; Curzons, A. D.; Constable, D. J. C.; Cunningham, V. L. *Clean Technol. Environ. Policy* **2004**, *7*, 42–50; (g) Gani, R.; Jiménez-González, C.; Constable, D. J. *Comput. Chem. Eng.* **2005**, *29*, 1661–1676.
20. *For some papers discussing the base effect*; (a) Košmrlj, J.; Maes, B. U. W.; Lemièrre, G. L. F.; Haemers, A. *Synlett* **2000**, 1581–1584; (b) Jonckers, T. H. M.; Maes, B. U. W.; Lemièrre, G. L. F.; Dommissie, R. *Tetrahedron* **2001**, *57*, 7027–7034; (c) Meyers, C.; Maes, B. U. W.; Loones, K. T. J.; Bal, G.; Lemièrre, G. L. F.; Dommissie, R. *J. Org. Chem.* **2004**, *69*, 6010–6017; (d) Yadav, A. K.; Verbeeck, S.; Hostyn, S.; Franck, P.; Sergeev, S.; Maes, B. U. W. *Org. Lett.* **2013**, *15*, 1060–1063; (e) Surry, D. S.; Buchwald, S. L. *Chem. Sci.* **2011**, *2*, 27–50.
21. *For examples on the use of metal catalysis on amino acids and peptides*; (a) Ruan, Z.; Sauer-  
mann, N.; Manoni, E.; Ackermann, L. *Angew. Chemie Int. Ed.* **2017**, *56*, 3172–3176; (b)  
Willemse, T.; Van Imp, K.; Goss, R. J. M.; Van Vlijmen, H. W. T.; Schepens, W.; Maes, B.  
U. W.; Ballet, S. *ChemCatChem* **2015**, *7*, 2055–2070; (c) Reay, A. J.; Hammarback, L. A.; Bray, J.  
T. W.; Sheridan, T.; Turnbull, D.; Whitwood, A. C.; Fairlamb, I. J. S. *ACS Catal.* **2017**, *7*, 5174–  
5179; (d) Skogh, A.; Friis, S. D.; Skrydstrup, T.; Sandström, A. *Org. Lett.* **2017**, *19*, 2873–2876;

- 1  
2 (e) Andersen, T. L.; Nordeman, P.; Christoffersen, H. F.; Audrain, H.; Antoni, G.; Skrydstrup, T.  
3  
4 *Angew. Chemie Int. Ed.* **2017**, *56*, 4549–4553.  
5  
6  
7 22. Basel, Y.; Hassner, A. *J. Org. Chem.* **2000**, *65*, 6368–6380.  
8  
9  
10 23. *For examples of development and use of this parameter*; (a) Abraham, M. H.; Abraham, R. J.;  
11  
12 Acree, W. E.; Aliev, A. E.; Leo, A. J.; Whaley, W. L. *J. Org. Chem.* **2014**, *79*, 11075–11083; (b)  
13  
14 Abraham, M. H.; Abraham, R. J.; Byrne, J.; Griffiths, L. *J. Org. Chem.* **2006**, *71*, 3389–3394; (c)  
15  
16 Abraham, M. H.; Abraham, R. J. *New J. Chem.* **2017**, *41*, 6064–6066.  
17  
18  
19 24. Koch, U.; Popelier, P. L. A. *J. Phys. Chem.* **1995**, *99*, 9747–9754.  
20  
21  
22 25. *For some examples*; (a) Gedye, R.; Rank, W.; Westaway, K. C. *Can. J. Chem.* **1991**, *69*, 706–711; (b)  
23  
24 Ko, S.; Han, H.; Chang, S. *Org. Lett.* **2003**, *5*, 2687–2690; (c) Ontoria, J. M.; Martín Hernando, J. I.;  
25  
26 Malancona, S.; Attenni, B.; Stansfield, I.; Conte, I.; Ercolani, C.; Habermann, J.; Ponzi, S.; Di  
27  
28 Filippo, M.; Koch, U.; Rowley, M.; Narjes, F. *Bioorg. Med. Chem. Lett.* **2006**, *16*, 4026–4030; (d)  
29  
30 van der Heijden, G.; Jong, J. A. W.; Ruijter, E.; Orru, R. V. A. *Organic Letters* **2016**, *18*, 984–987.  
31  
32  
33 26. *For transamidation of N-Boc- or N-Ts-activated secondary amides*; (a) Liu, Y.; Shi, S.; Achten-  
34  
35 hagen, M.; Liu, R.; Szostak, M. *Org. Lett.* **2017**, *19*, 1614–1617.  
36  
37  
38 27. *For examples in transition metal-catalyzed directed C-H activation making use of the 8-*  
39  
40 *aminoquinoline auxiliary*; (a) Roane, J.; Daugulis, O. *J. Am. Chem. Soc.* **2016**, *138*, 4601–4607; (b)  
41  
42 Roane, J. *Encycl. Reagents Org. Synth.*; John Wiley & Sons, Ltd: Chichester, UK, 2015; pp 1–17; (c)  
43  
44 Wei, Y.; Tang, H.; Cong, X.; Rao, B.; Wu, C.; Zeng, X. *Org. Lett.* **2014**, *16*, 2248–2251.  
45  
46  
47 28. Zaitsev, V. G.; Shabashov, D.; Daugulis, O. *J. Am. Chem. Soc.* **2005**, *127*, 13154–13155.  
48  
49  
50 29. Shabashov, D.; Daugulis, O. *J. Am. Chem. Soc.* **2010**, *132*, 3965–3972.  
51  
52  
53 30. Tran, L. D.; Roane, J.; Daugulis, O. *Angew. Chemie Int. Ed.* **2013**, *52*, 6043–6046.  
54  
55  
56  
57  
58  
59  
60

## Graphical TOC Entry



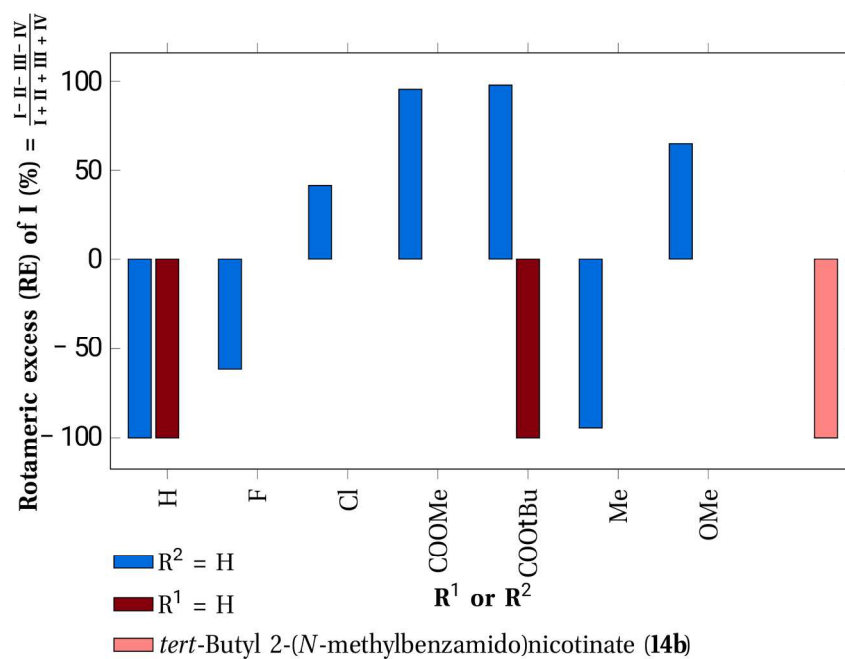
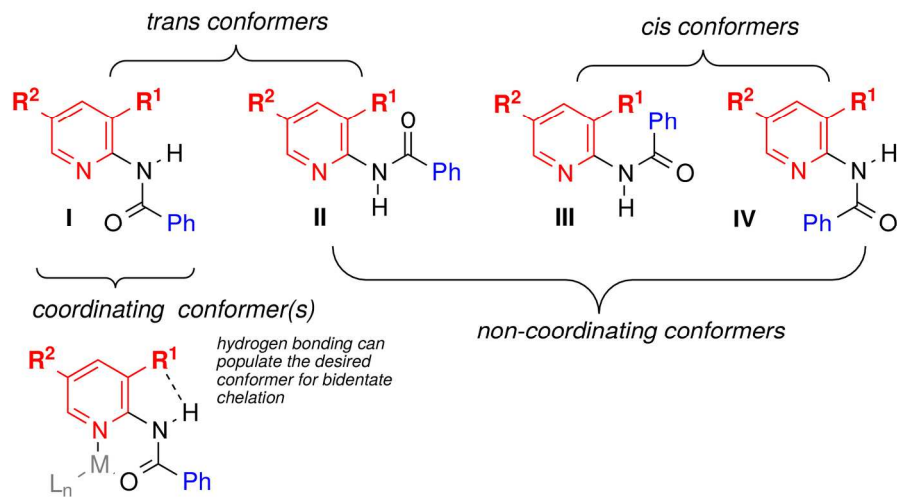


Figure 1

184x242mm (300 x 300 DPI)

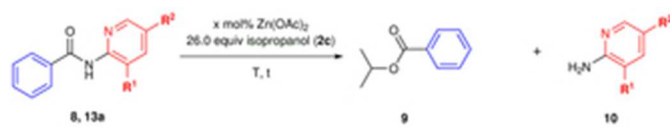


Figure 2 (TOP)

28x5mm (300 x 300 DPI)

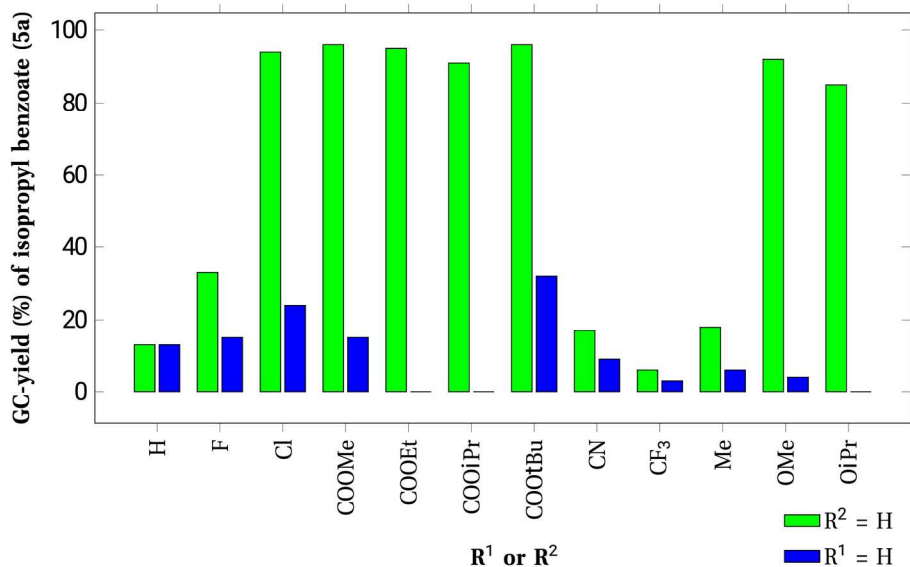
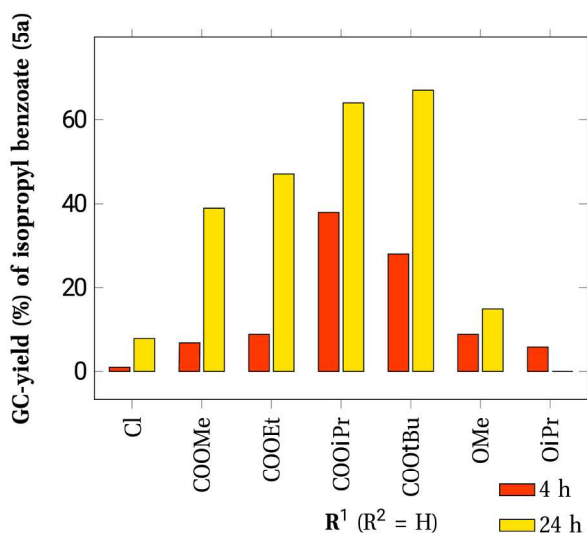
(a) 25 mol% Zn(OAc)<sub>2</sub>, 75° C, 6 h.(b) 10 mol% Zn(OAc)<sub>2</sub>, 40° C, 4 h and 24 h.

Figure 2 (BOTTOM)

204x273mm (300 x 300 DPI)

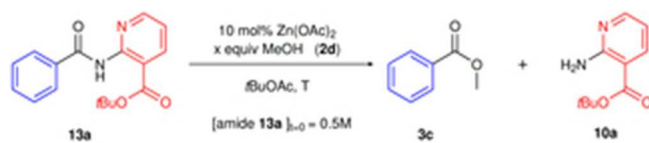


Figure 3 (TOP)

27x5mm (300 x 300 DPI)

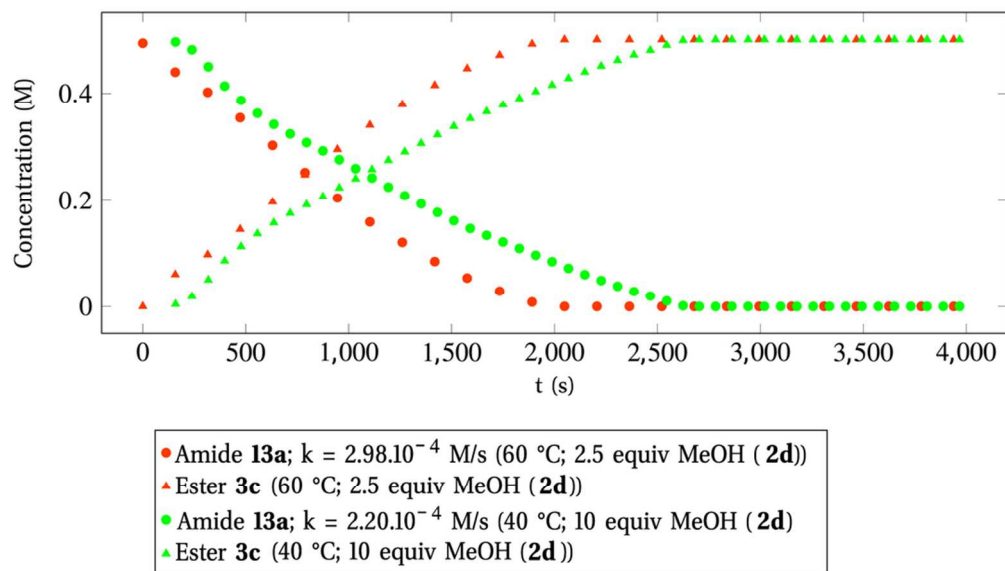


Figure 3 (MIDDLE)

91x52mm (300 x 300 DPI)

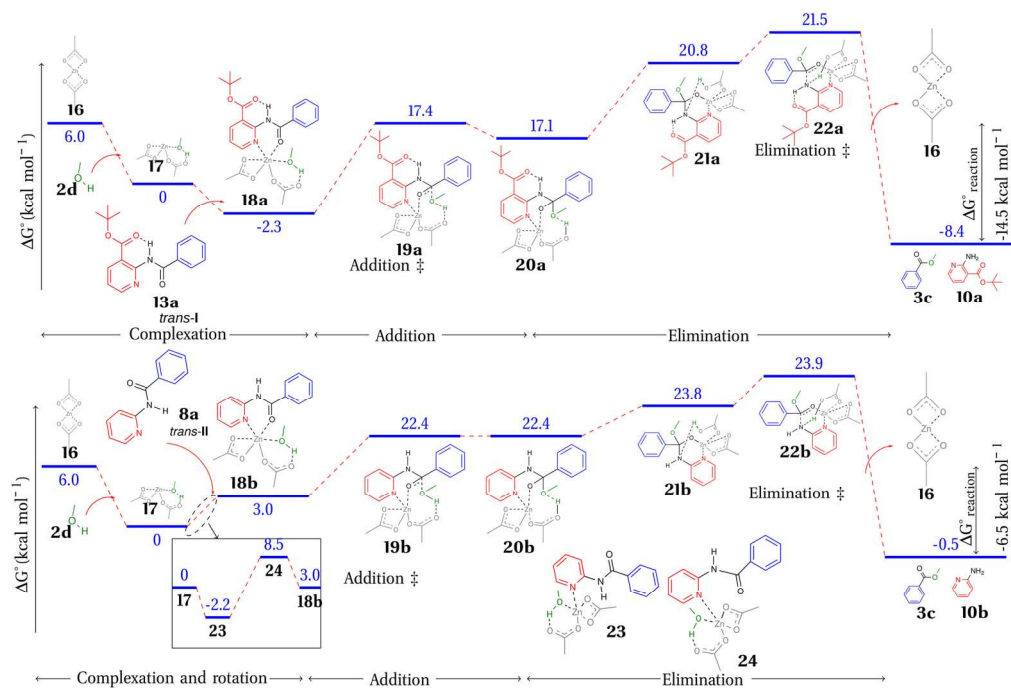
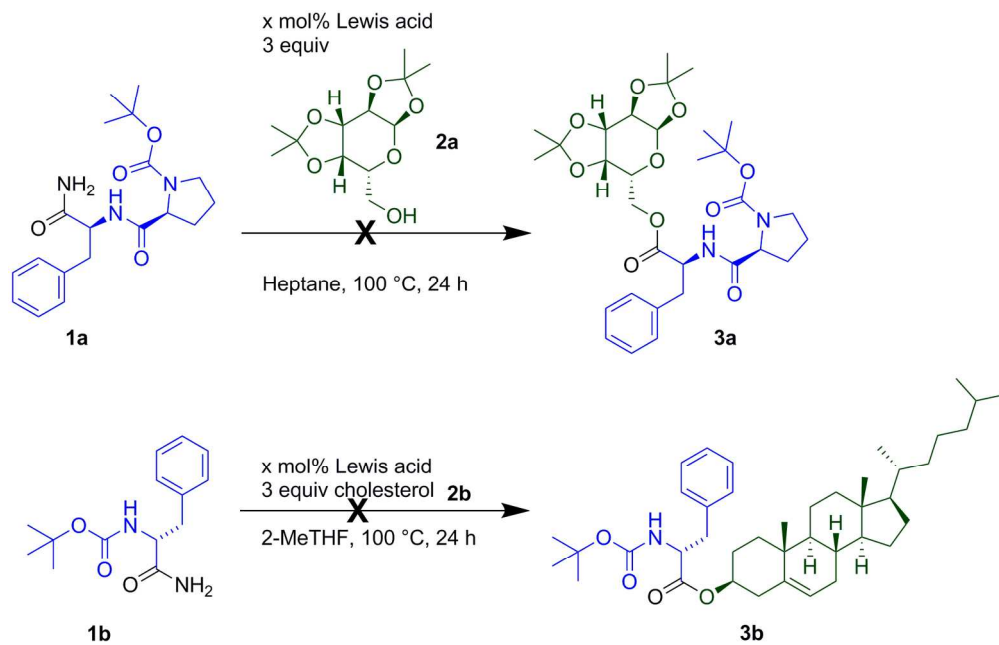


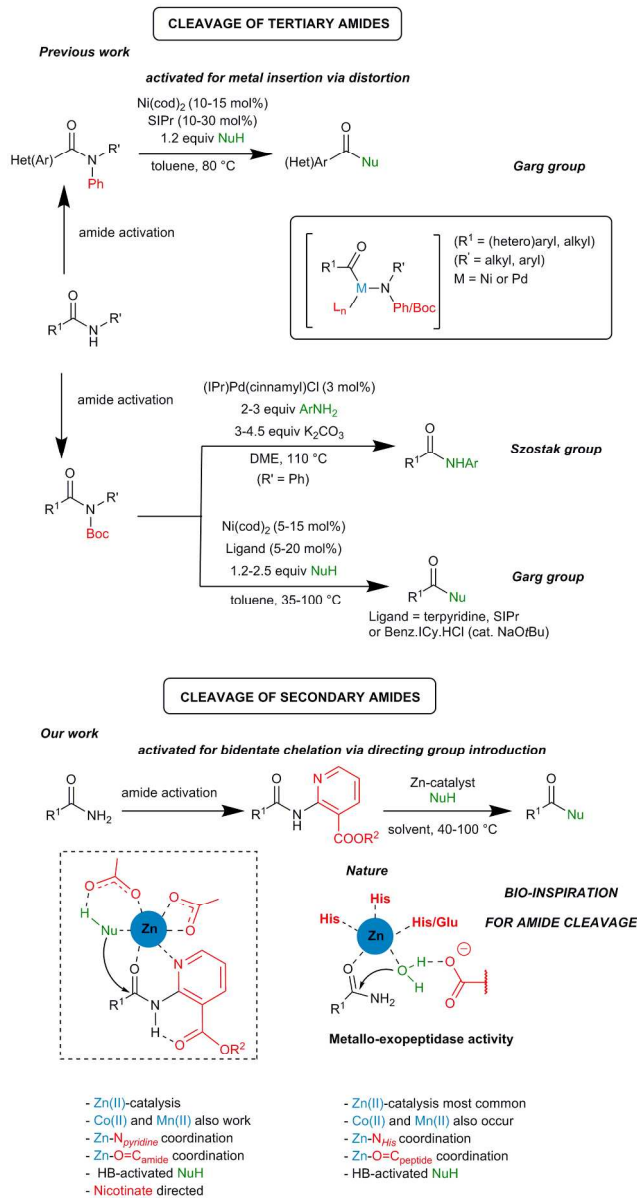
Figure 4

160x108mm (300 x 300 DPI)



Scheme 1

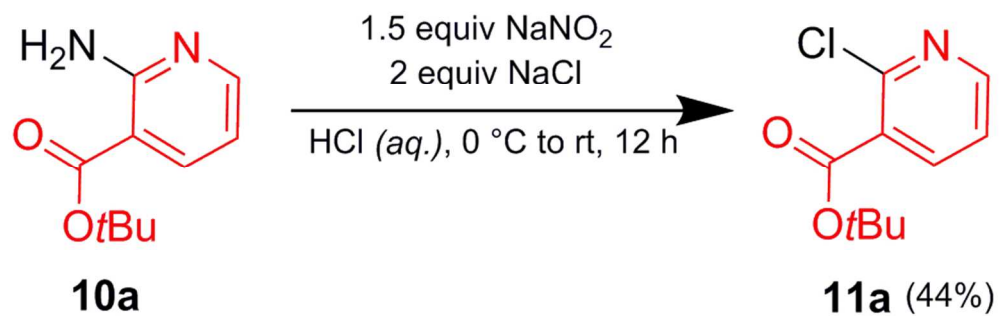
170x109mm (300 x 300 DPI)



Scheme 2

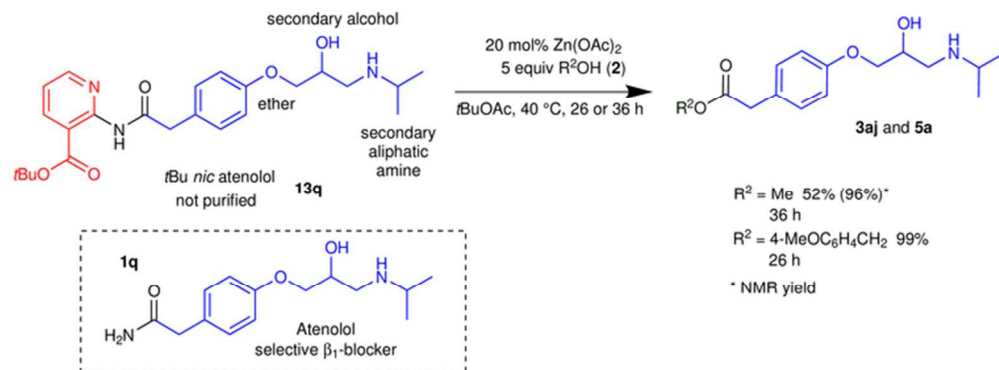
134x255mm (300 x 300 DPI)





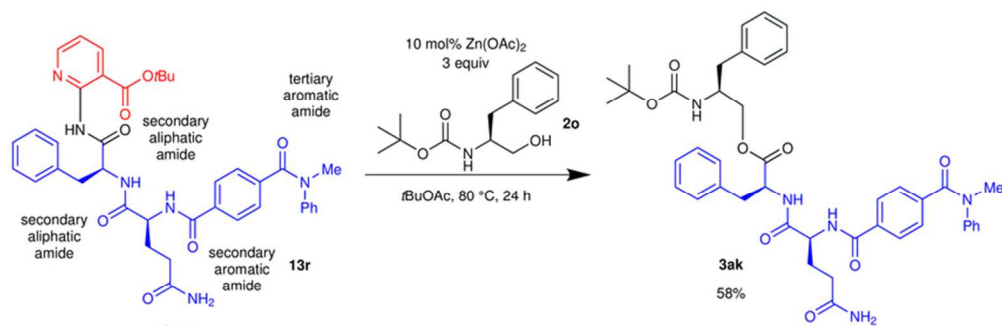
Scheme 4

84x27mm (300 x 300 DPI)



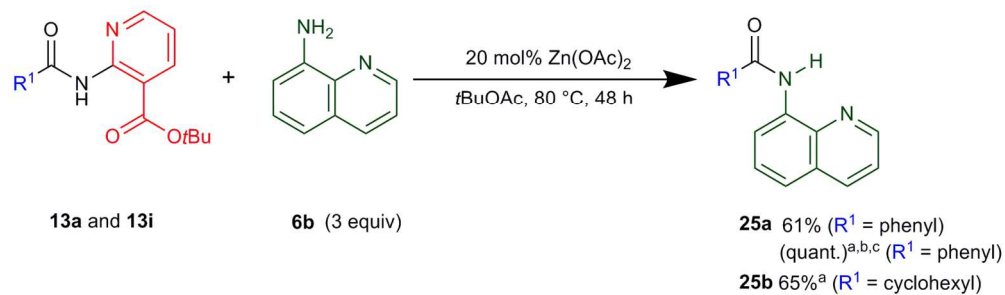
Scheme 5 top

64x24mm (300 x 300 DPI)



Scheme 5 bottom

72x26mm (300 x 300 DPI)



Scheme 6

142x41mm (300 x 300 DPI)

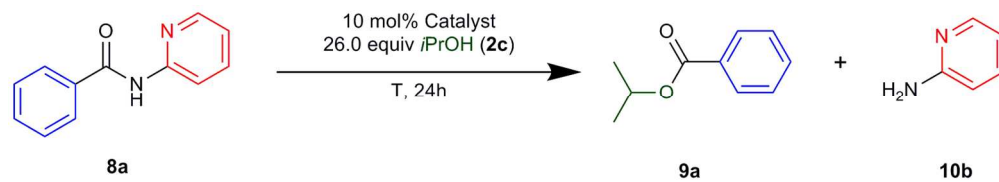


Table 1

143x26mm (300 x 300 DPI)

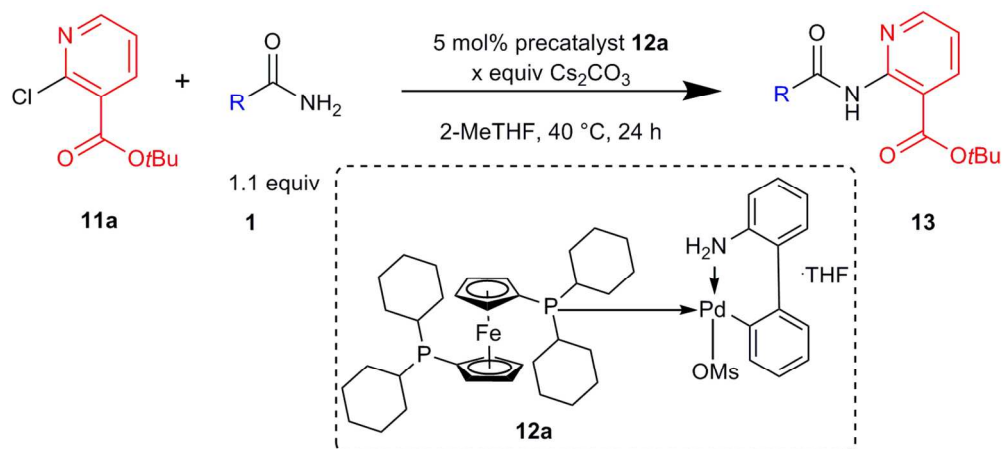


Table 2

124x56mm (300 x 300 DPI)

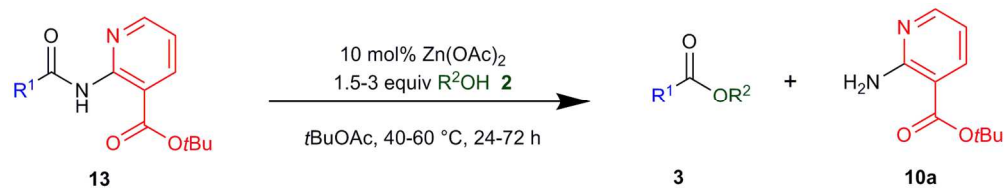


Table 3

142x27mm (300 x 300 DPI)



Table 4

142x27mm (300 x 300 DPI)

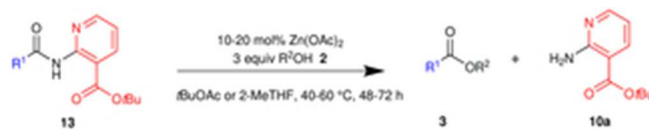


Table 5

27x5mm (300 x 300 DPI)

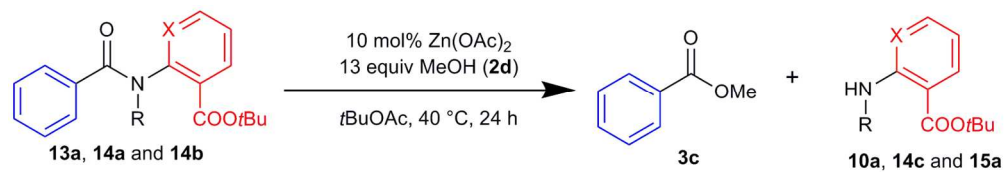


Table 6

142x24mm (300 x 300 DPI)

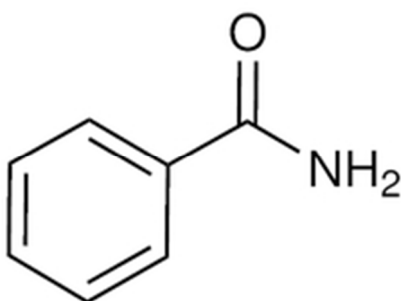


Table 2 entry 1 compound 1c

17x13mm (300 x 300 DPI)

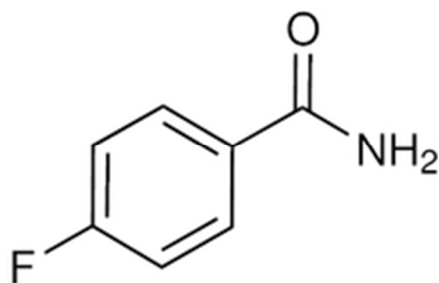


Table 2 entry 2 compound 1d

19x13mm (300 x 300 DPI)

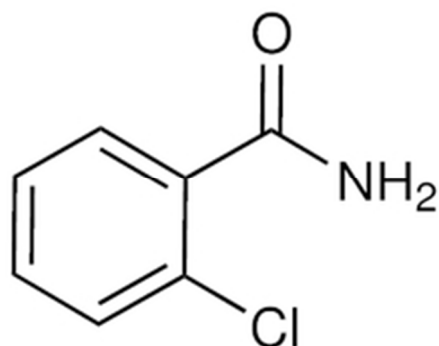


Table 2 entry 3 compound 1e

19x15mm (300 x 300 DPI)

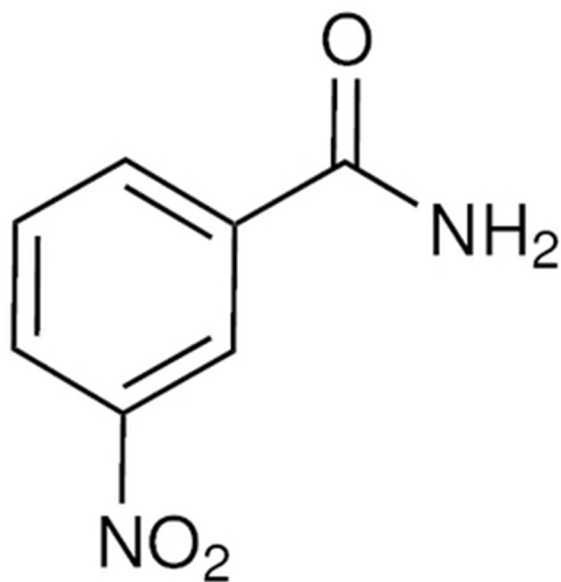


Table 2 entry 4 compound 1f

24x26mm (300 x 300 DPI)

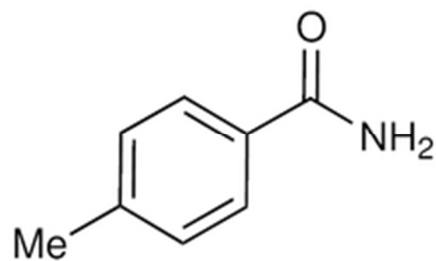


Table 2 entry 5 compound 1g

19x11mm (300 x 300 DPI)

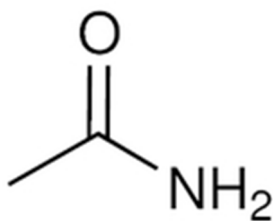


Table 2 entry 6 compound 1h

12x10mm (300 x 300 DPI)

1  
2  
3  
4  
5  
6  
7  
8  
9  
10  
11  
12  
13  
14  
15  
16  
17  
18  
19  
20  
21  
22  
23  
24  
25  
26  
27  
28  
29  
30  
31  
32  
33  
34  
35  
36  
37  
38  
39  
40  
41  
42  
43  
44  
45  
46  
47  
48  
49  
50  
51  
52  
53  
54  
55  
56  
57  
58  
59  
60

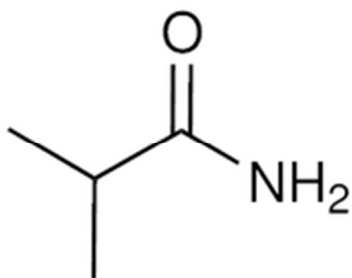


Table 2 entry 7 compound 1i

15x13mm (300 x 300 DPI)

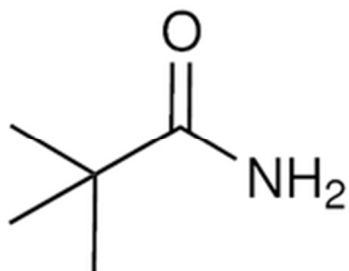


Table 2 entry 8 compound 1j

15x12mm (300 x 300 DPI)

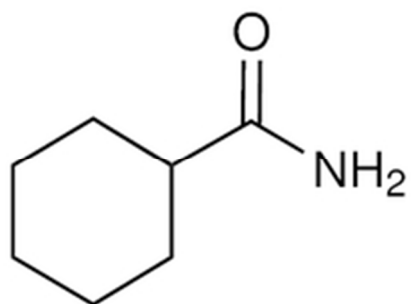


Table 2 entry 9 compound 1k

18x13mm (300 x 300 DPI)

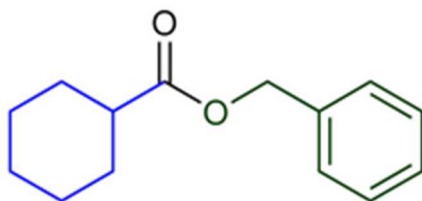


Table 3 entry 1 compound 3d

18x9mm (300 x 300 DPI)

1  
2  
3  
4  
5  
6  
7  
8  
9  
10  
11  
12  
13  
14  
15  
16  
17  
18  
19  
20  
21  
22  
23  
24  
25  
26  
27  
28  
29  
30  
31  
32  
33  
34  
35  
36  
37  
38  
39  
40  
41  
42  
43  
44  
45  
46  
47  
48  
49  
50  
51  
52  
53  
54  
55  
56  
57  
58  
59  
60

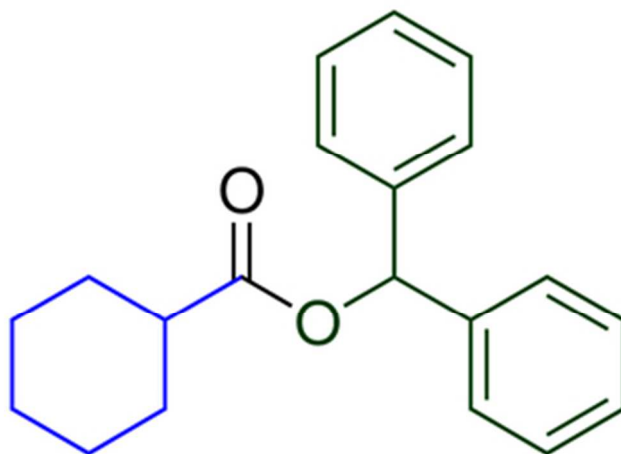


Table 3 entry 2 compound 3e

27x20mm (300 x 300 DPI)

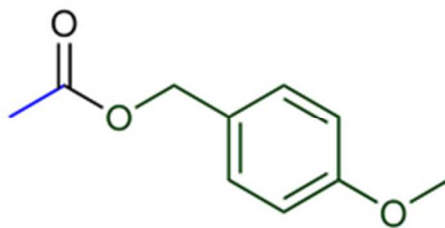


Table 3 entry 3 compound 3f

19x10mm (300 x 300 DPI)

1  
2  
3  
4  
5  
6  
7  
8  
9  
10  
11  
12  
13  
14  
15  
16  
17  
18  
19  
20  
21  
22  
23  
24  
25  
26  
27  
28  
29  
30  
31  
32  
33  
34  
35  
36  
37  
38  
39  
40  
41  
42  
43  
44  
45  
46  
47  
48  
49  
50  
51  
52  
53  
54  
55  
56  
57  
58  
59  
60

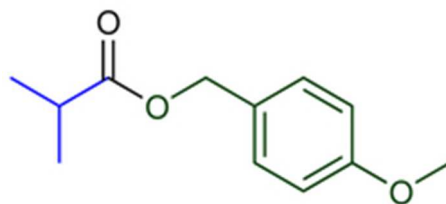


Table 3 entry 4 compound 3g

19x9mm (300 x 300 DPI)

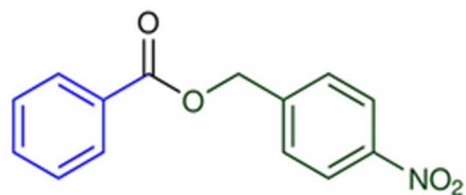


Table 3 entry 5 compound 3h

19x8mm (300 x 300 DPI)

1  
2  
3  
4  
5  
6  
7  
8  
9  
10  
11  
12  
13  
14  
15  
16  
17  
18  
19  
20  
21  
22  
23  
24  
25  
26  
27  
28  
29  
30  
31  
32  
33  
34  
35  
36  
37  
38  
39  
40  
41  
42  
43  
44  
45  
46  
47  
48  
49  
50  
51  
52  
53  
54  
55  
56  
57  
58  
59  
60

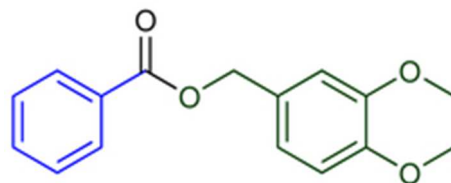


Table 3 entry 6 compound 3i

19x8mm (300 x 300 DPI)

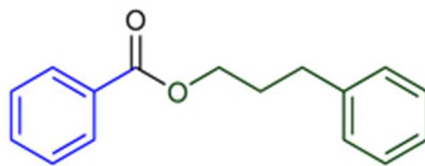


Table 3 entry 7 compound 3j

18x7mm (300 x 300 DPI)

1  
2  
3  
4  
5  
6  
7  
8  
9  
10  
11  
12  
13  
14  
15  
16  
17  
18  
19  
20  
21  
22  
23  
24  
25  
26  
27  
28  
29  
30  
31  
32  
33  
34  
35  
36  
37  
38  
39  
40  
41  
42  
43  
44  
45  
46  
47  
48  
49  
50  
51  
52  
53  
54  
55  
56  
57  
58  
59  
60

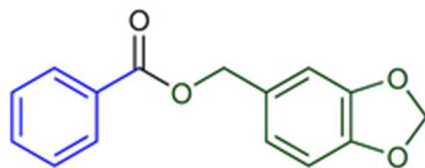


Table 3 entry 8 compound 3k

18x7mm (300 x 300 DPI)

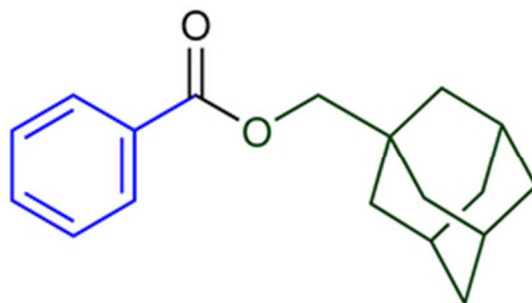


Table 3 entry 9 compound 31

23x13mm (300 x 300 DPI)

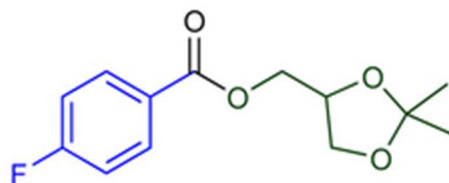


Table 3 entry 10 compound 3m

19x8mm (300 x 300 DPI)

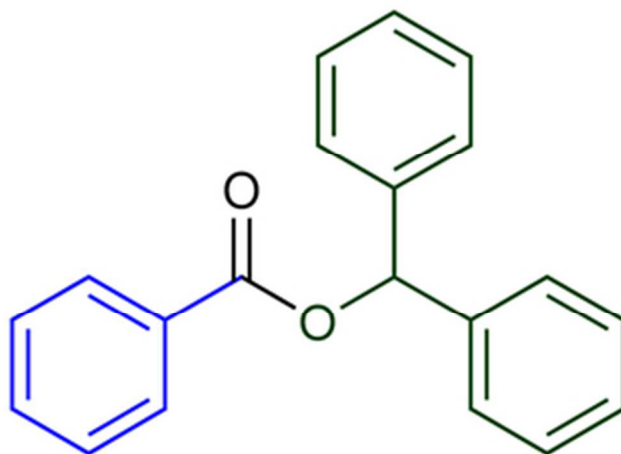


Table 3 entry 11 compound 3n

27x20mm (300 x 300 DPI)

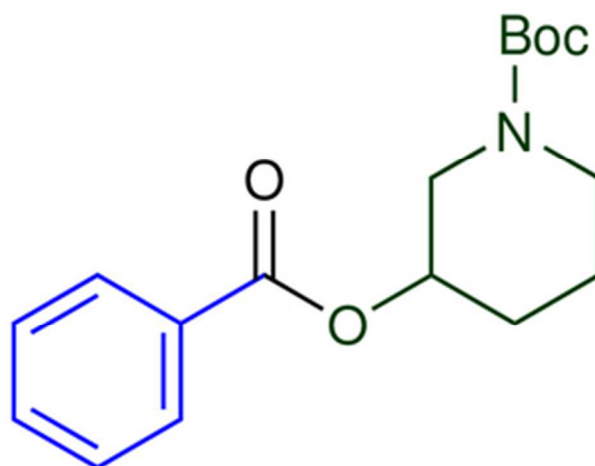


Table 3 entry 12 compound 30

26x20mm (300 x 300 DPI)

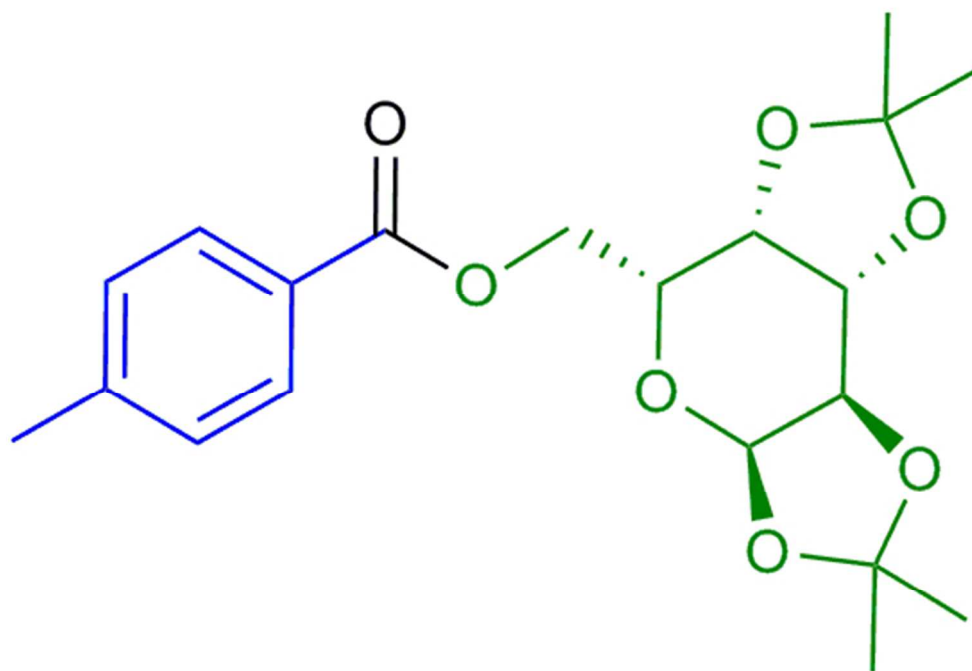


Table 4 entry 1  
Compound 3p

47x32mm (300 x 300 DPI)

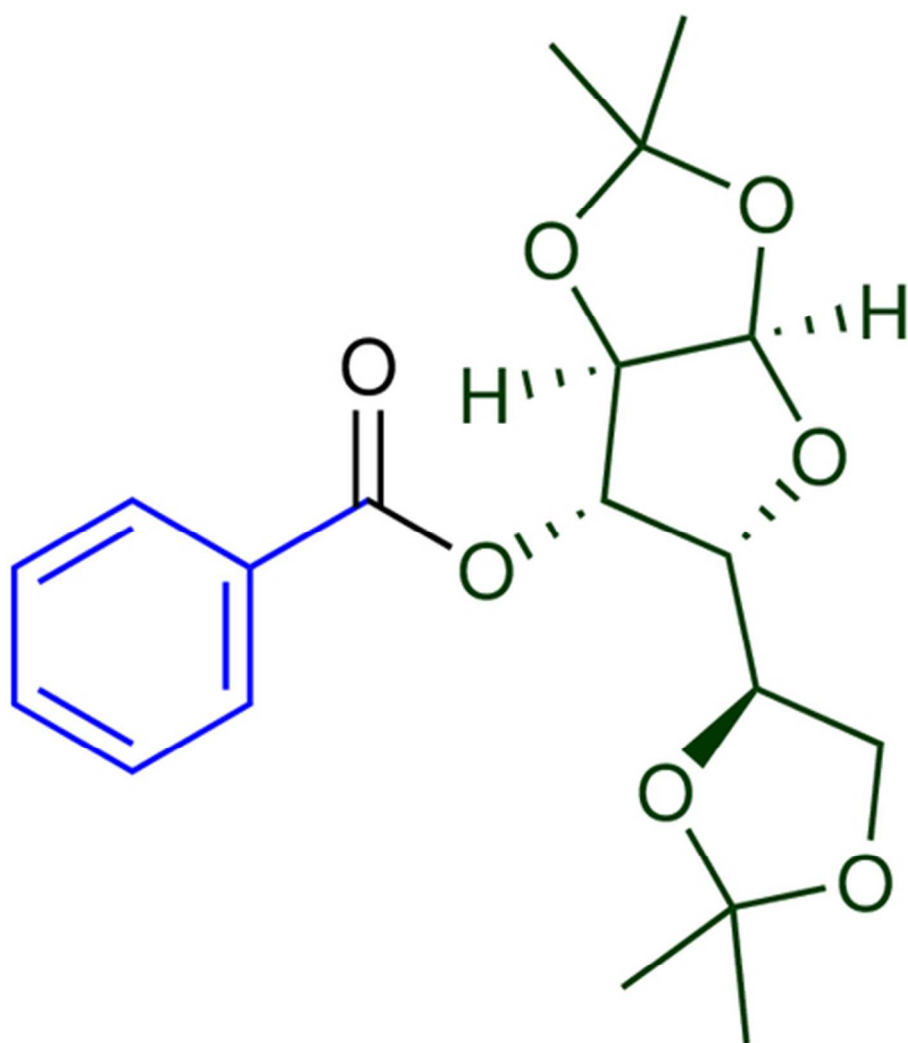


Table 4 entry 2 compound 3q

40x45mm (300 x 300 DPI)

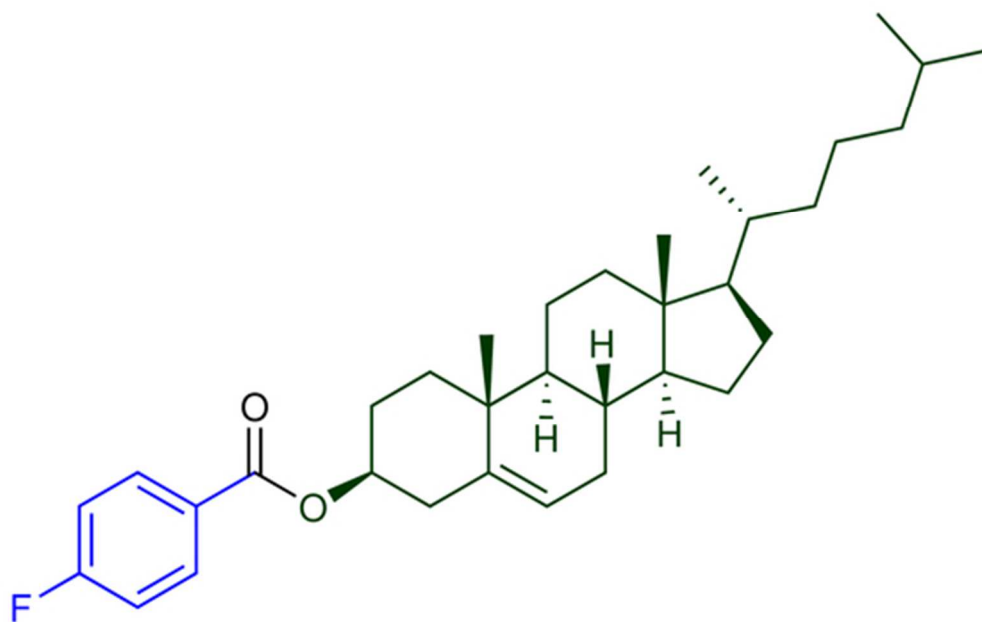


Table 4 entry 3 compound 3r

47x30mm (300 x 300 DPI)

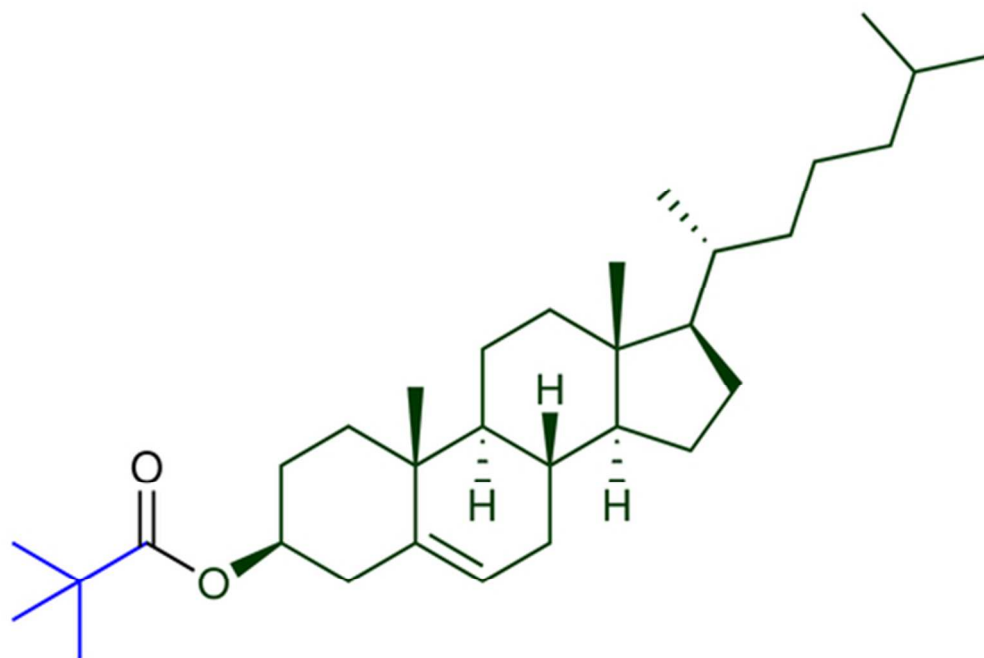


Table 4 entry 4 compound 3s

44x30mm (300 x 300 DPI)

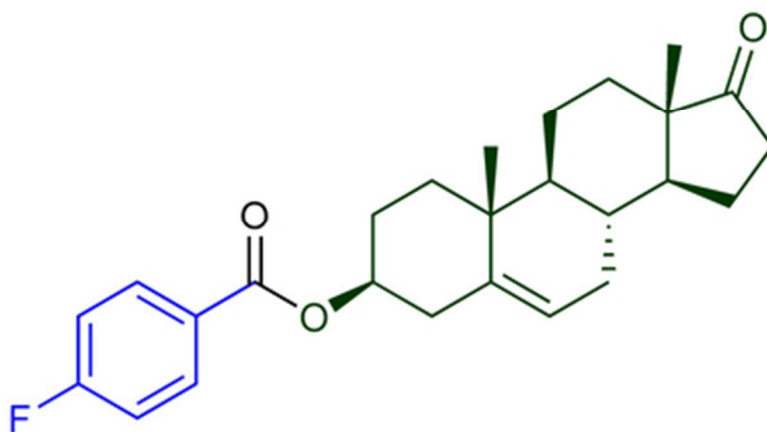


Table 4 entry 5 compound 3t

33x18mm (300 x 300 DPI)

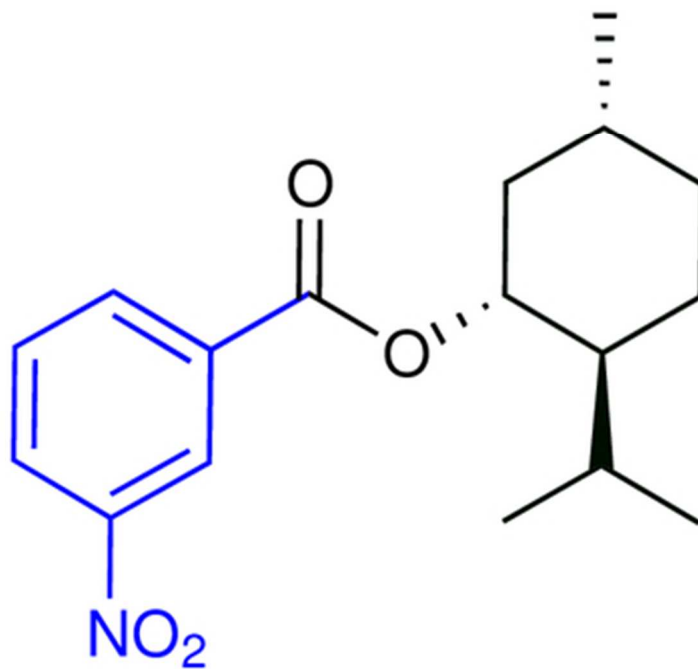


Table 4 entry 6 compound 3u

30x29mm (300 x 300 DPI)

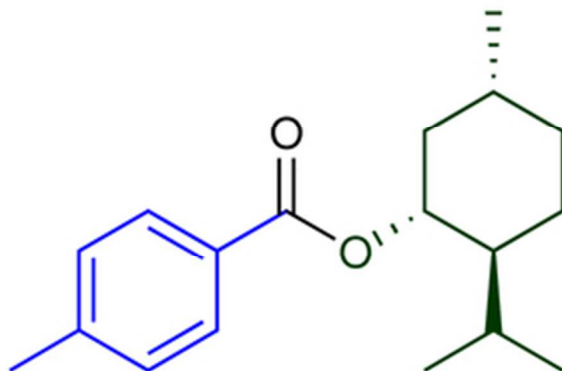


Table 4 entry 7 compound 3v

24x16mm (300 x 300 DPI)

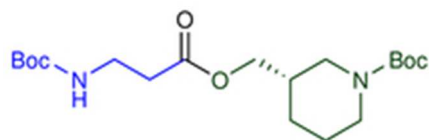


Table 4 entry 8 compound 3w

18x6mm (300 x 300 DPI)

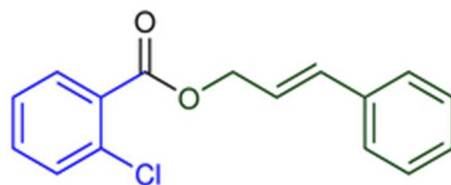


Table 4 entry 9 compound 3x

19x8mm (300 x 300 DPI)

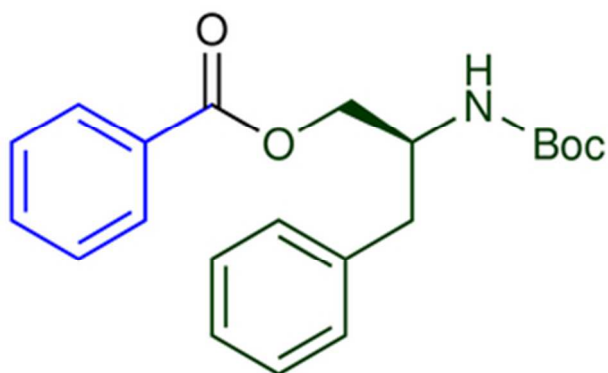


Table 5 entry 1 compound 3y

26x16mm (300 x 300 DPI)

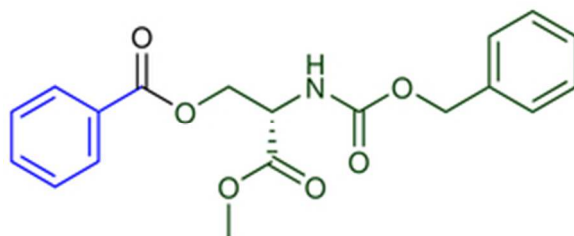


Table 5 entry 2 compound 3z

24x10mm (300 x 300 DPI)

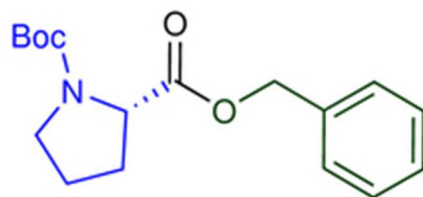


Table 5 entry 3 compound 3aa

18x8mm (300 x 300 DPI)

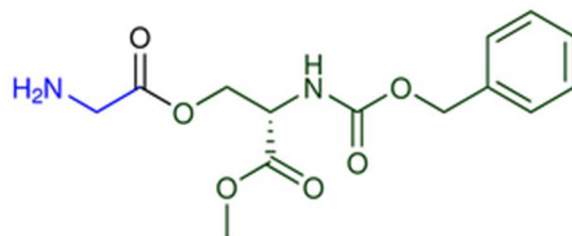


Table 5 entry 4 compound 3ab

24x10mm (300 x 300 DPI)

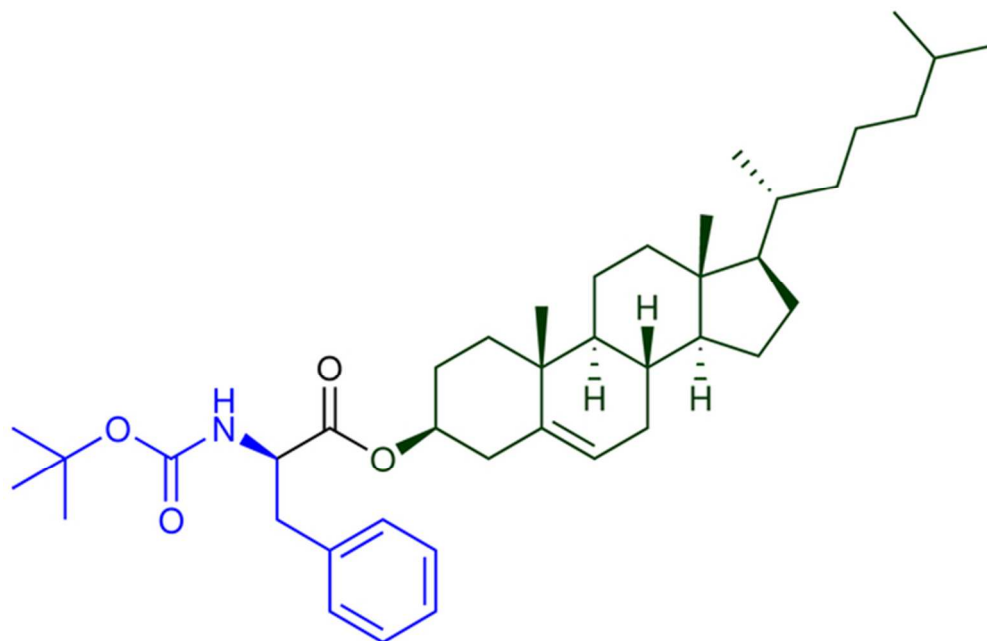


Table 5 entry 5 compound 3b

54x35mm (300 x 300 DPI)

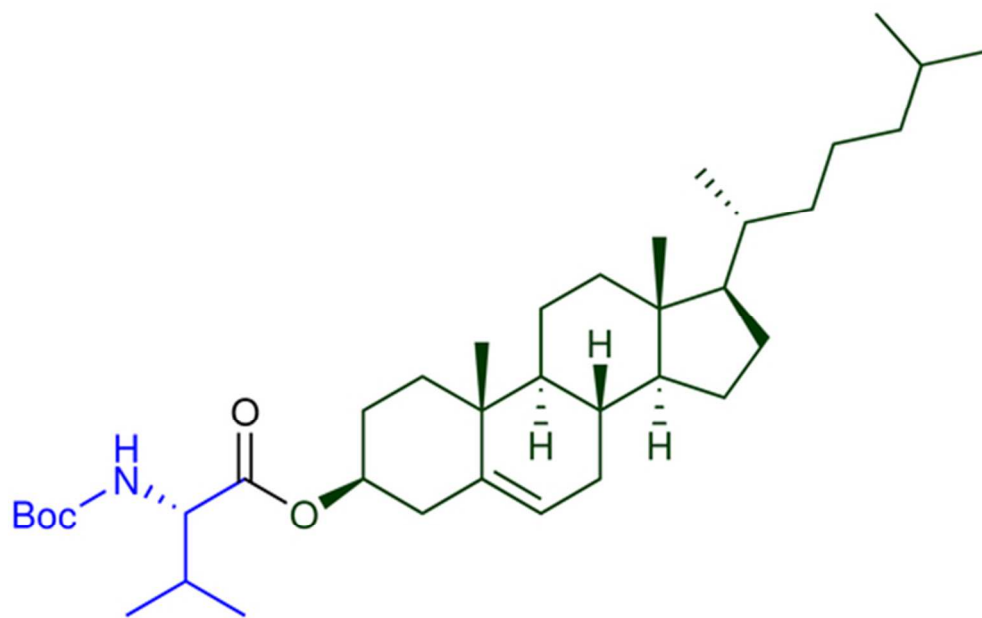


Table 5 entry 6 compound 3ac

46x29mm (300 x 300 DPI)

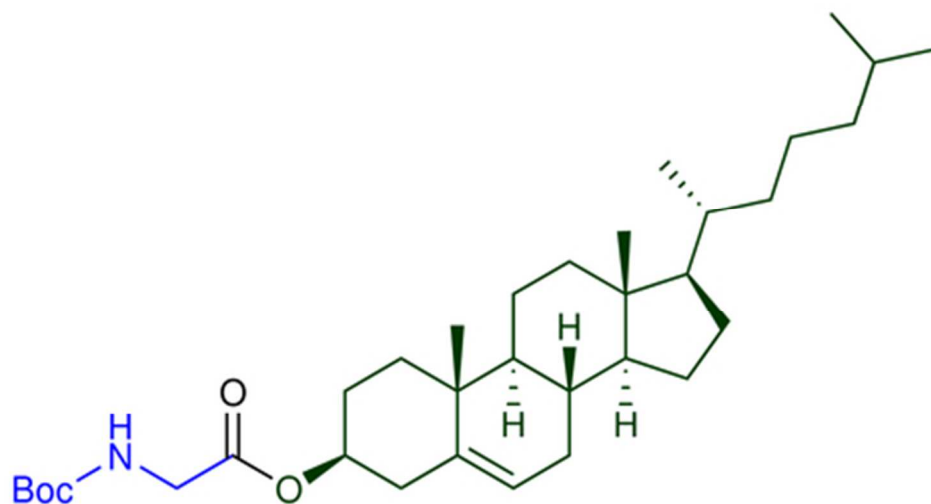


Table 5 entry 7 compound 3ad

40x21mm (300 x 300 DPI)

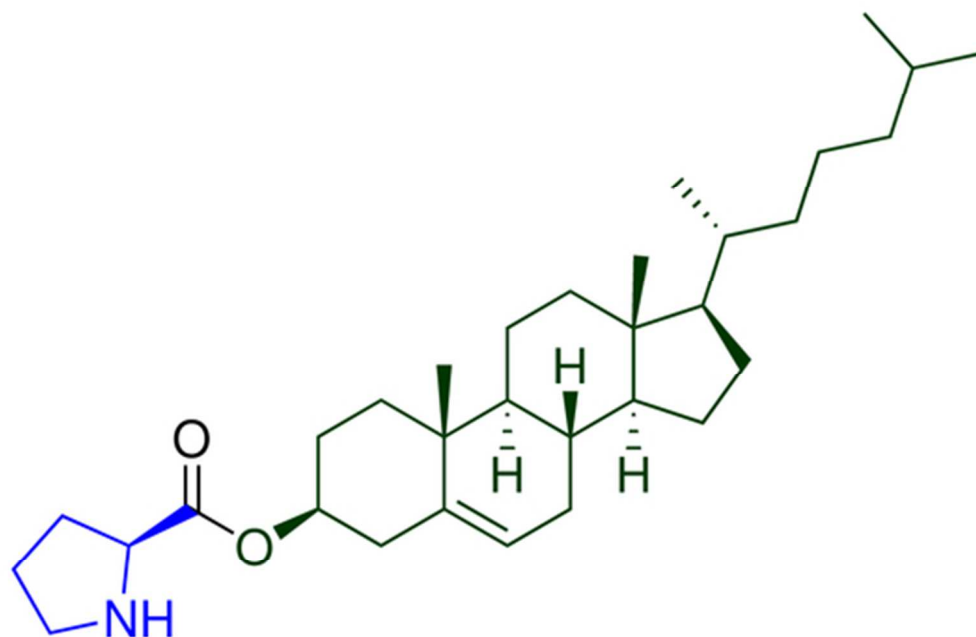


Table 5 entry 8 compound 3ae

45x29mm (300 x 300 DPI)

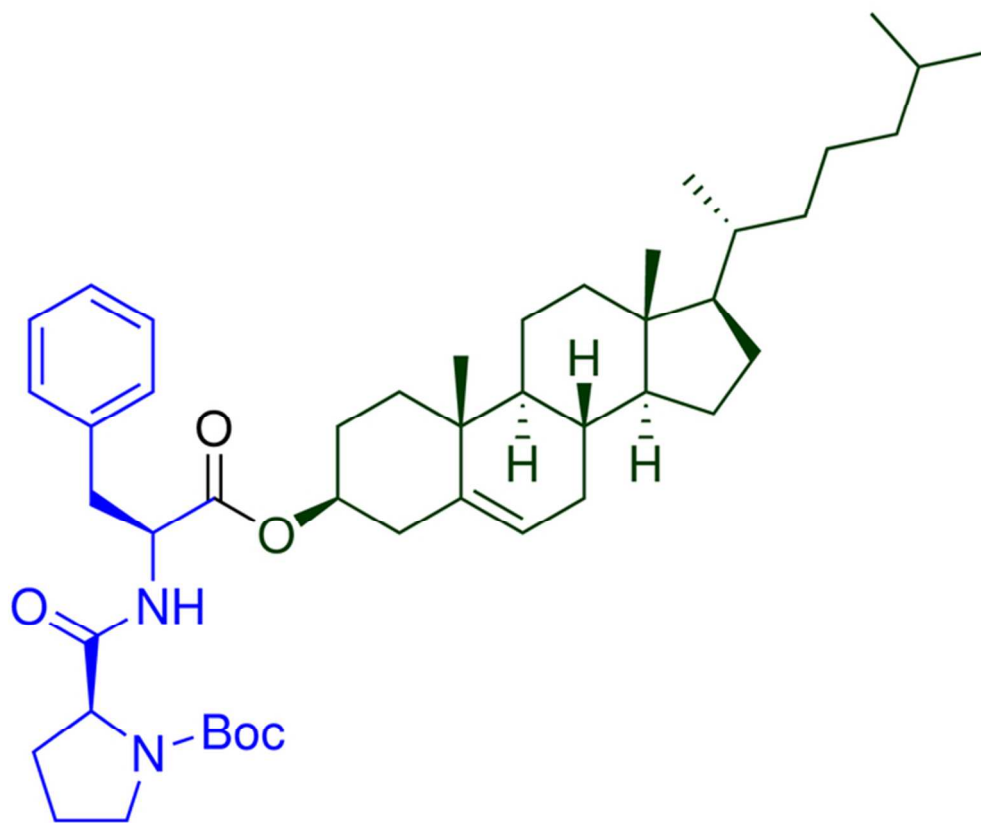


Table 5 entry 9 compound 3af

59x49mm (300 x 300 DPI)

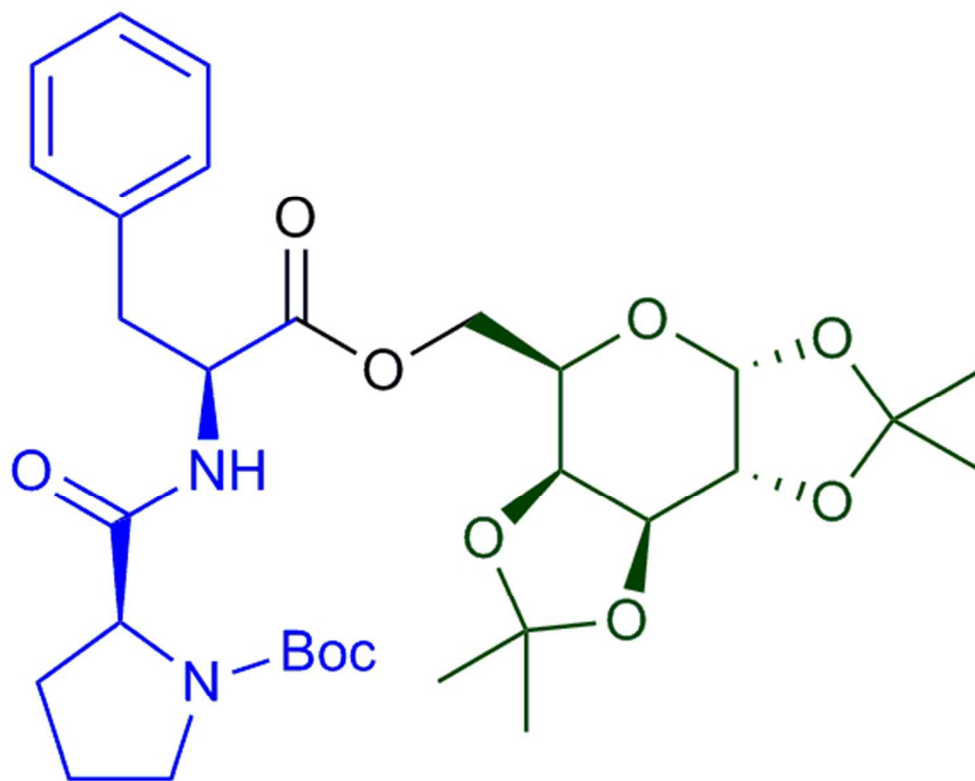


Table 5 entry 10!! + Compound 3a

49x39mm (300 x 300 DPI)

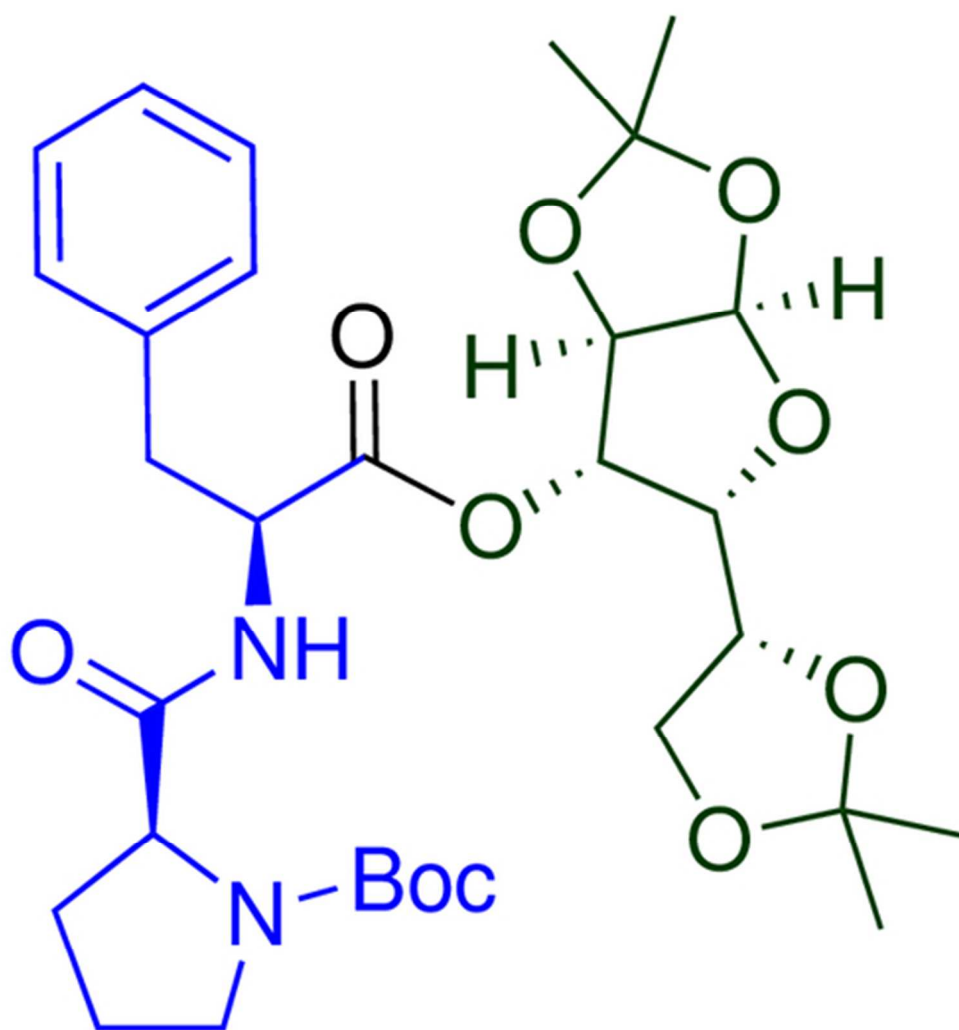


Table 5 entry 11 compound 3ag

43x45mm (300 x 300 DPI)

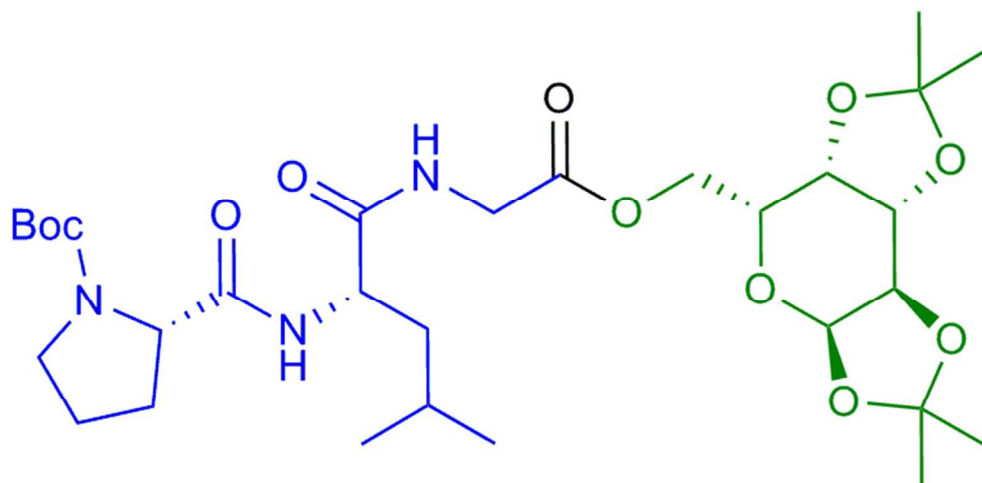


Table 5 entry 12 Compound 3ah

65x32mm (300 x 300 DPI)

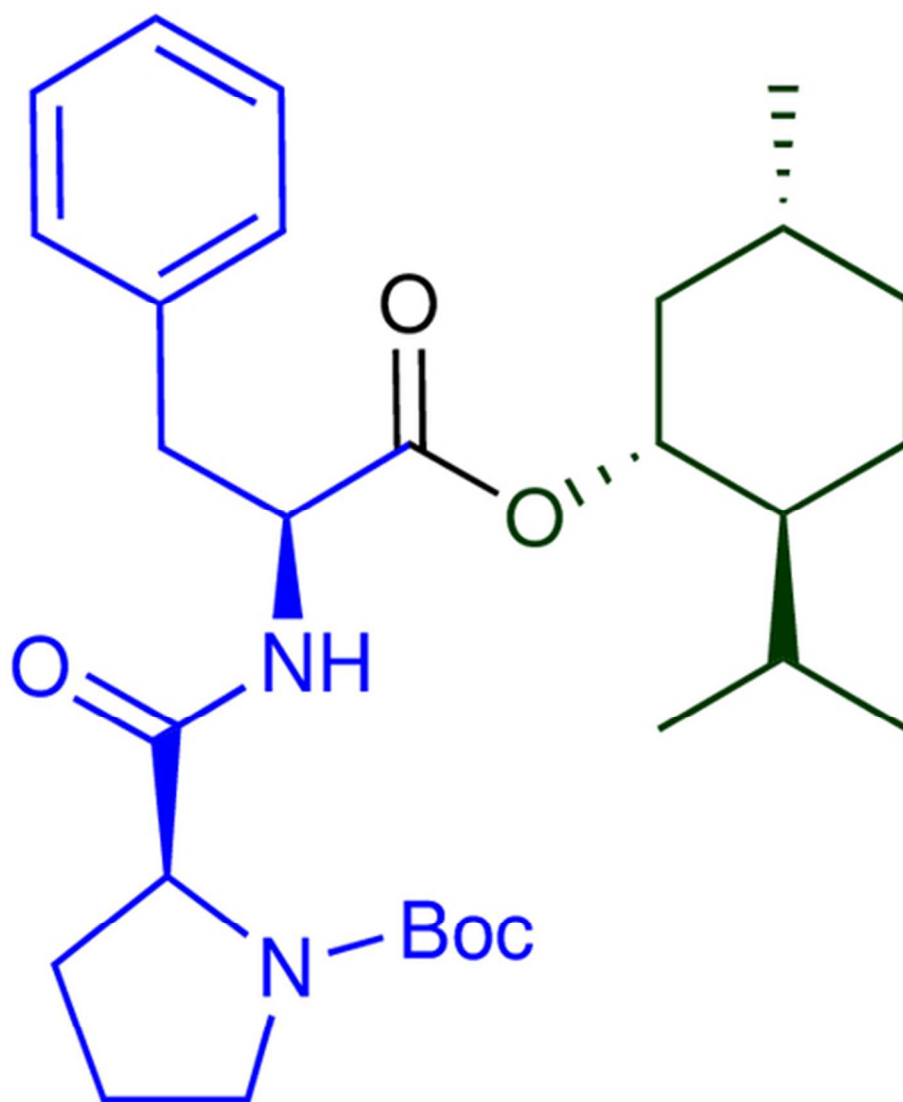
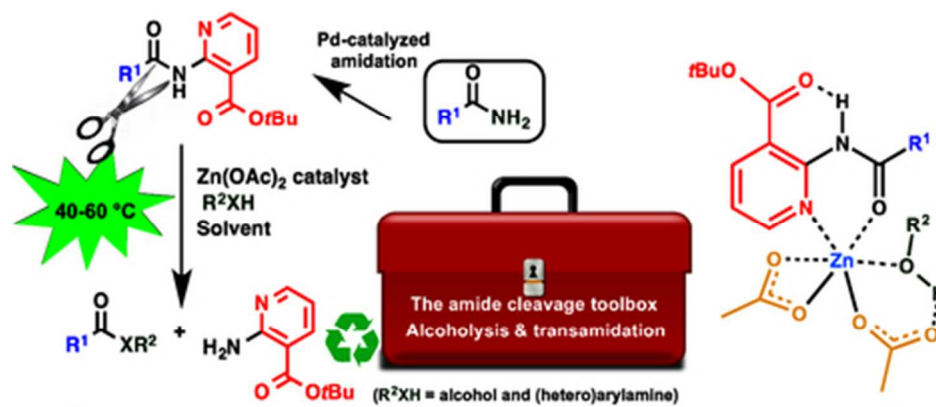


Table 5 entry 13 compound 3ai

40x48mm (300 x 300 DPI)



graphical abstract

40x17mm (300 x 300 DPI)